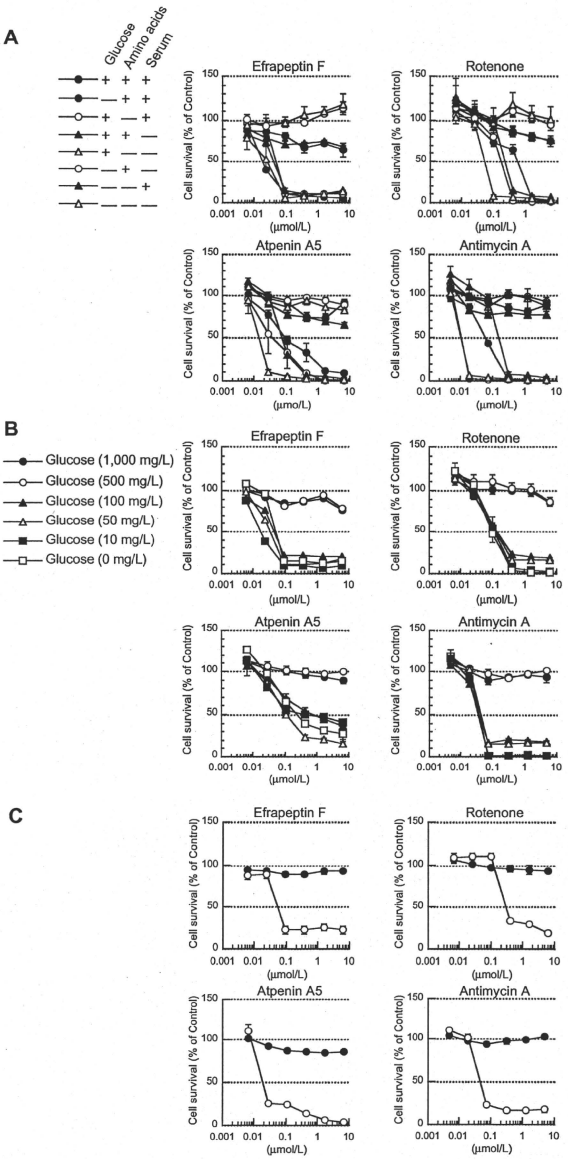
A
Glucose
Amino acids
Serum
Efrapeptin F
Rotenone
Atpenin A5
Antimycin A
Cell survival (% of Control)
(μmol/L)
B
Glucose (1,000 mg/L)
Glucose (500 mg/L)
Glucose (100 mg/L)
Glucose (50 mg/L)
Glucose (10 mg/L)
Glucose (0 mg/L)
C

Materials and methods

Inhibitors. Efrapeptin F and Atpenin A_5 were purified from microbial culture extracts supplied by Meiji Seika Kaisha in our laboratory [15–18]. Rotenone and antimycin A were obtained from Sigma–Aldrich (St. Louis, MO).

Cell lines and culture conditions. Human pancreatic cancer PANC-1 cells and prostate cancer PC-3 cells were obtained from the American Type Culture Collection (Rockville, MD). Cells were grown at 37 °C with 5% CO_2 in Dulbecco's modified Eagle medium (DMEM; Nissui, Tokyo, Japan) supplemented with 10% fetal bovine serum (FBS; Tissue Culture Biologicals, Tulare, CA), 100,000 U/L penicillin G, and 100 mg/L streptomycin. Nutrient starvation was achieved by culturing cells in nutrient-deprived medium (NDM) as previously described [9]. Briefly, the NDM composition was 265 mg/L $CaCl_2{\cdot}H_2O$, 400 mg/L KCl, 200 mg/L $MgSO_4{\cdot}7H_2O$, 6400 mg/L NaCl, 163 mg/L $NaH_2PO_4{\cdot}2H_2O$, 0.1 mg/L $Fe(NO_3)_3{\cdot}9H_2O$, 5 mg/L phenol red, 100,000 U/L penicillin G, 100 mg/L streptomycin, 25 mmol/L HEPES buffer (pH 7.4), and MEM vitamin solution (Invitrogen, Carlsbad, CA); the final pH was adjusted to 7.4 with 10% $NaHCO_3$.

Preferential cytotoxicity in nutrient-deprived conditions. PANC-1 cells (2.5×10^4 cells/well) in 96-well plates were cultured in DMEM (10% FBS) for 24 h. The cells were washed with PBS and the medium was replaced with either fresh DMEM (10% FBS) or NDM (−). Test samples were added to the well and cells were cultured for 24 h. Furthermore, the medium was replaced with DMEM (10% FBS) containing 0.5 mg/mL thiazolyl blue tetrazolium bromide (MTT; Sigma–Aldrich) and incubated for 3 h to determine cytotoxicity using the MTT assay [19]. Hypoxia was achieved by culturing cells with a mixture of 1% O_2, 5% CO_2 and 94% N_2.

Measurement of cellular ATP content. PANC-1 cells (2.5×10^4 cells/well) in 96-well plates were cultured in DMEM (10% FBS) for 24 h. The cells were washed with PBS and cultured in fresh DMEM (10% FBS) or NDM (−) with 0.25 μmol/L rotenone, 0.27 μmol/L atpenin A_5, 0.10 μmol/L antimycin A or 0.06 μmol/L efrapeptin F for 24 h. The ATP level in cells was determined using the CellTiter-Glo Luminescent Cell Viability Assay (Promega, Madison, WI).

Flow cytometric analysis. PANC-1 cells (5×10^5) in 60-mm dishes were incubated in DMEM (10% FBS) for 24 h. The cells were washed with PBS and the medium was replaced with either fresh DMEM (10% FBS) or NDM (−). Mitochondrial inhibitors (0.1 μmol/L) were added to the well and the cells were cultured for 24 h. The cells were incubated with annexin V-FITC and propidium iodide according to an annexin V-FITC apoptosis detection kit (Biovision Research Products, Mountain View, CA) and analyzed using a flow cytometer (FACSCalibur; BD Biosciences, Franklin Lakes, NJ).

Animal experiments. Male severe combined immunodeficient (SCID) mice, 6 weeks old, were purchased from Charles River Japan (Yokohama, Japan) and maintained in a specific pathogen-free barrier facility according to our institutional guidelines. PC-3 cells (1×10^7) were subcutaneously injected into the SCID mouse in the left lateral flank. Five days after inoculation, mice were divided randomly into test groups (control $n = 9$, efrapeptin F-treated $n = 7$) and efrapeptin F was intravenously administered twice weekly for 3 weeks to the efrapeptin F-treated group. Cisplatin was intravenously administered once weekly for 3 weeks. Tumor volume was estimated using the following formula: tumor volume (mm^3) = (length × $width^2$)/2.

Statistical analysis. All data are representative of three independent experiments with similar results. The statistical data are expressed as mean ± SD using descriptive statistics. Statistical analysis was done by using Student's *t*-test.

Results

Efrapeptin F is preferentially cytotoxic to cancer cells in nutrient-deprived conditions

To identify cytotoxic agents that function preferentially on nutrient-deprived cancer cells, we screened the cultured media from various microorganisms. One extract of microbial cultured media exhibited preferential cytotoxicity to PANC-1 cells in nutrient-deprived medium (NDM (−)). The extract was subjected to chromatography to obtain a pure compound. The NMR and MS spectra data revealed its chemical structure to be efrapeptin F (Fig. 1A) [15,16]. Efrapeptin F exhibited preferential cytotoxicity to PANC-1 cells in NDM (−), but not in nutrient-sufficient medium (DMEM (10% FBS)) (Fig. 1B). The cytotoxic effect of efrapeptin F on PANC-1 cells in NDM (−) (IC_{50} = 0.052 μmol/L) was more than 100 times stronger than in DMEM (10% FBS) (IC_{50} = >10 μmol/L).

Mitochondrial inhibitors are preferentially cytotoxic to cancer cells in nutrient-deprived conditions

Efrapeptin F has been previously reported to act as an inhibitor of mitochondrial F_1F_0-ATPase (complex V) [17]. Therefore, we examined whether mitochondrial complex V inhibitors function as cytotoxic agents preferentially on nutrient-deprived cells (Fig. 1B). Interestingly, leucinostatin A and oligomycin (complex V inhibitors) were more cytotoxic to PANC-1 cells in NDM (−) compared with DMEM (10% FBS) [20,21]. In addition, rotenone and piericidin A_1 (NADH-ubiquinone reductase (complex I) inhibitors), atpenin A_5 (a succinate-ubiquinone reductase (complex II) inhibitor), antimycin A, stigmatellin and myxothiazol (ubiquinone-cytochrome *c* (complex III) inhibitors) also were more cytotoxic to PANC-1 cells in NDM (−) compare to DMEM (10% FBS) (Fig. 1C) [20–22]. These results clearly demonstrate that mitochondrial inhibitors exhibit preferential cytotoxicity to nutrient-deprived PANC-1 cells. Efrapeptin F (a complex V inhibitor), rotenone (a complex I inhibitor), atpenin A_5 (a complex II inhibitor), and antimycin A (a complex III inhibitor) were selected for further study. The mode of cell death caused by mitochondrial inhibitors in nutrient-deprived conditions was examined using annexin V-FITC and propidium iodide double staining and flow cytometry. Mitochondrial inhibitors significantly increased the early-apoptotic and late-apoptotic cells in nutrient-deprived conditions, but not to nutrient-sufficient conditions (Fig. 1D). These results suggested that these inhibitors induce apoptosis in nutrient-deprived cells.

Mitochondrial inhibitors are preferentially cytotoxic to cancer cells only under glucose-limiting conditions

To determine what nutrient component was responsible for cytotoxicity of mitochondrial inhibitors, we examined the effect

Fig. 2. Effect of mitochondrial inhibitors on PANC-1 survival under glucose-starved conditions and hypoxic conditions. (A) Effect of nutrient starvation on cytotoxicity of mitochondrial inhibitors. PANC-1 cells were incubated with inhibitors in nutrient-deprived medium containing glucose, amino acids and/or dialyzed FBS for 24 h. (B) Effect of glucose levels on cytotoxicity of mitochondrial inhibitors. PANC-1 cells were incubated with inhibitors in DMEM (10% dialyzed FBS) containing the indicated concentrations of glucose for 24 h. (C) Effect of hypoxia on cytotoxicity of mitochondrial inhibitors. PANC-1 cells were incubated with inhibitors in DMEM (10% FBS) (●) or NDM (−) (○) under 1% O_2 for 24 h.

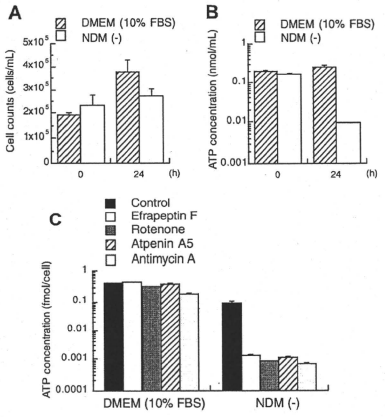

Fig. 3. Effect of mitochondrial inhibitors on cellular ATP levels of PANC-1 cells grown in nutrient-deprived medium. (A) Effect of nutrient starvation on PANC-1 cell growth. PANC-1 cells were incubated in DMEM (10% FBS) or NDM (−) for 24 h and cell numbers were measured by cell counting. (B) Cellular ATP levels were determined by the CellTiter-Glo Luminescent Cell Viability Assay after incubation in DMEM (10% FBS) or NDM (−) for 24 h. (C) PANC-1 cells were incubated with 0.25 μmol/L rotenone, 0.27 μmol/L atpenin A_5, 0.10 μmol/L antimycin A and 0.06 μmol/L efrapeptin F in DMEM (10% FBS) or NDM (−) for 24 h and cellular ATP levels were determined.

of these inhibitors on PANC-1 cell survival under various nutrient-starved conditions (Fig. 2A). Mitochondrial inhibitors preferentially induced cell death under glucose-deprived conditions, irrespective of the presence or absence of amino acids and/or serum. We then examined the effect of glucose levels on cytotoxicity of these inhibitors (Fig. 2B). The concentration of glucose in DMEM is 1000 mg/L. Mitochondrial inhibitors did not induce cell death in the PANC-1 cells cultured with 1000 and 500 mg/L glucose, but in less than 100 mg/L glucose each inhibitor exhibited cytotoxicity. These results demonstrate clearly that glucose is the key component to determine the sensitivity of cancer cells to mitochondrial inhibitors.

Mitochondrial inhibitors are preferentially cytotoxic to nutrient-deprived cells under hypoxic conditions

Because large areas of tumor are exposed not only to nutrient starvation but also to hypoxic conditions, we examined preferential cytotoxicity of mitochondrial inhibitors to nutrient-deprived cells in hypoxic conditions (Fig. 2C). These inhibitors were more cytotoxic to nutrient-deprived PANC-1 cells in 1% O_2 as well as 21% O_2. Our results demonstrate that mitochondrial inhibitors show preferentially cytotoxicity to nutrient-deprived cells not only under normoxic conditions but also under hypoxic conditions.

Reduction of cellular ATP levels by mitochondrial inhibitors induces preferential cell death to nutrient-deprived cells

To investigate why mitochondrial inhibitors exhibit preferential cytotoxicity to nutrient-deprived cells, we examined the effect of mitochondrial inhibitors on cellular ATP levels in nutrient-deprived cells. When PANC-1 cells were incubated in NDM (−) for 24 h, the cells grew less and the cellular ATP levels were markedly decreased (Fig. 3A and B). Since PANC-1 cells incubated in NDM (−) for 24 h could hardly be stained by trypan blue, the cells were able to survive in nutrient starvation in spite of lower ATP levels (Fig. S1). When PANC-1 cells were exposed to mitochondrial inhibitors for 24 h, the amount of cellular ATP were slightly decreased in DMEM (10% FBS), whereas in NDM (−) cellular ATP content decreased 100-fold compared to controls (Fig. 3C). These results indicate that depletion of ATP exerts preferential cytotoxicity to nutrient-starved cells.

Table 1
Growth inhibitory activity of efrapeptin F against 39 human cancer cell lines in the JFCR39 panel.

Origin of cancer	Cell line	Log GI_{50} (μmol/L)[a]
Breast	HBC-4	−7.22
	BSY-1	−6.73
	HBC-5	−8.00
	MCF-7	−8.00
	MDA-MB-231	−5.94
Central nervous system	U251	−7.45
	SF-268	−6.17
	SF-295	−8.00
	SF-539	−6.13
	SNB-75	−5.79
	SNB-78	−6.47
Colon	HCC2998	−6.84
	KM-12	−6.65
	HT-29	−6.86
	HCT-15	−5.61
	HCT-116	−6.48
Lung	NCI-H23	−8.00
	NCI-H226	−6.60
	NCI-H522	−8.00
	NCI-H460	−6.69
	A549	−6.53
	DMS273	−6.64
	DMS114	−8.00
Melanoma	LOX-IMVI	−6.71
Ovary	OVCAR-3	−6.58
	OVCAR-4	−5.85
	OVCAR-5	−6.21
	OVCAR-8	−8.00
	SK-OV-3	−6.46
Kidney	RXF-631L	−5.17
	ACHN	−5.94
Stomach	St-4	−6.10
	MKN1	−6.56
	MKN7	−8.00
	MKN28	−8.00
	MKN45	−6.78
	MKN74	−8.00
Prostate	DU-145	−6.76
	PC-3	−8.00
MG-MID[b]		−6.87
Delta[c]		1.13
Range[d]		2.83

[a] Log concentration of efrapeptin F for inhibition of cell growth at 50% compared to control.
[b] Mean value of log GI_{50} over all cell lines tested.
[c] The difference in log GI_{50} value of the most sensitive cell and MG-MID value.
[d] The difference in log GI_{50} value of the most sensitive cell and the least sensitive cell.

Efrapeptin F inhibits tumor growth in vivo

PANC-1 cells are low tumorigenicity even in immunodeficient mice. To explore the *in vivo* antitumor activity of mitochondrial inhibitors, we examined the growth inhibitory activity of efrapeptin F against 39 human cancer cell lines of the JFCR39 panel (Table 1) [23–25]. Efrapeptin F exhibited potent growth inhibitory

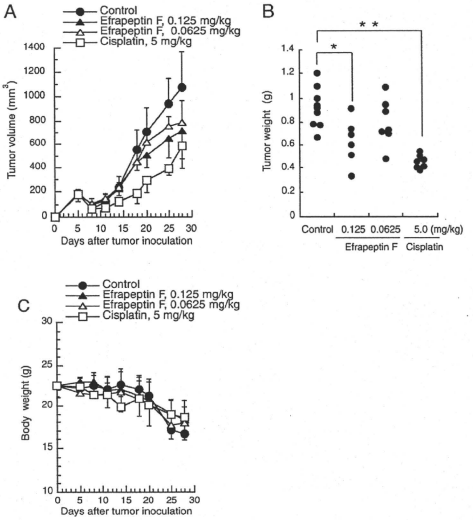

Fig. 4. Antitumor effect of efrapeptin F on PC-3 cells in SCID mice. PC-3 cells (1×10^7) were subcutaneously inoculated into SCID mice on day 0. Efrapeptin F was administrated intravenously twice weekly for 3 weeks from day 5. (A) Tumor volumes. *Y* axis, tumor volume (mm^3); *X* axis, time (day). (B) Tumor weight. The tumors were excised on day 28. $^{**}P < 0.001$; $^{*}P < 0.05$, compared with control (Student's *t*-test). (C) Body weight. *Y* axis, body weight (g); *X* axis, time (day). *Points*, mean values; *bars*, SD.

activity, and the mean value for log concentration for inhibition of cell growth at 50% compared to control was −6.87 (135 μmol/L). In particular, HBC-5, MCF-7, SF-295, NCI-H23, NCI-H522, DMS114, OVCAR-8, MKN7, MKN28, MKN74 and PC-3 cells were sensitive to efrapeptin F. Efrapeptin F showed preferential cytotoxicity to PC-3 cells in nutrient-deprived conditions as well as to PANC-1 cells (Fig. S2). Therefore, xenograft models of PC-3 cells were used to evaluate the *in vivo* antitumor activity of efrapeptin F. Efrapeptin F was intravenously administered twice weekly for 3 weeks from day 5 after the tumor inoculation. Efrapeptin F inhibited tumor growth of the PC-3 xenograft (Fig. 4A and B). Efrapeptin F at 0.125 and 0.0625 mg/kg reduced tumor weight by 68% and 86%, respectively (Tumor weight (g), control = 0.92 ± 0.17 (mean ± SD), 0.125 mg/kg efrapeptin F = 0.63 ± 0.20, 0.0625 mg/kg efrapeptin F = 0.79 ± 0.20) (Fig. 4B). To assess toxicity, we measured the body weight of the tumor-bearing mice (Fig. 4C). Their weight was not reduced by administration of efrapeptin F at these doses. However, among seven mice that were administrated efrapeptin F at a high dose (125 μg/kg), only one mouse died at day 23. Remaining mice survived until the end of the experiment without a decrease of body weight and anatomically without toxic effects in critical organs.

Discussion

Tumor microenvironment strongly affects tumor development and progression. Many aspects of physiology that differentiate solid tumors from normal tissues arise from differences in vasculature. Disorganized vascular systems in tumors result in large areas of tumor exposed to nutrient starvation and hypoxic conditions. In addition, due to the unregulated growth of tumor cells caused by genetic and epigenetic alterations, tumor cells proliferate more rapidly than normal cells and nutrient and oxygen demands often exceed supply [26–28]. In particular, highly aggressive tumor cells such as pancreatic cancers that are relatively hypovascular, are able to survive even in conditions of low nutrients and low oxygen supply. Since chronic nutrient deprivation seldom occurs in normal tissues, one strategy for anticancer agent development is to target cancer cells growing in nutrient-deprived conditions. Thus, we screened to identify cytotoxic agents that function preferentially in nutrient-deprived cancer cells.

Previous studies have shown that conventional chemotherapeutic drugs and various small molecule inhibitors were only weakly cytotoxic to cancer cells in nutrient-deprived conditions [9]. In this study, we found that the small molecule efrapeptin F, which is produced by some fungi showed preferential cytotoxicity to PANC-1 cells grown in nutrient-deprived conditions compared with cells in nutrient-sufficient conditions. Because efrapeptin F inhibits the mitochondrial complex V, we examined whether mitochondrial complex V inhibitors such as leucinostatin A and oligomycin act as cytotoxic agents preferentially on nutrient-deprived cells. Interestingly, these inhibitors were more cytotoxic to PANC-1 cells in NDM (−) compared to DMEM (10% FBS). In addition, mitochondrial complex I inhibitors (rotenone and piericidin A_1), a complex II inhibitor (atpenin A_5), and complex III inhibitors (antimycin A, stigmatellin and myxothiazol) also were more cytotoxic to PANC-1 cells in NDM (−). These results clearly demonstrate that mitochondrial inhibitors exhibit preferential cytotoxicity to nutrient-deprived PANC-1 cells, suggesting that mitochondrial inhibitors have unique and attractive characteristics in antitumor agent development. These inhibitors induced cell death under glucose-limiting conditions, irrespective of the presence or absence of amino acids and/or serum. The glucose concentration in colon cancers is only ~1 of 45 of typical plasma glucose concentration (1000 mg/L

or 5.6 nmol/L) [13]. Mitochondrial inhibitors did not induce cell death in 1000 mg/L glucose, but each inhibitors exhibited cytotoxicity in less than 100 mg/L glucose levels. The cytotoxicity caused by mitochondrial inhibitors depended on glucose levels in the culture medium and glucose was the key component to determine the sensitivity of cancer cells to their inhibitors. However, it is unclear how mitochondrial inhibitors exhibit preferential cytotoxicity to nutrient-deprived cells. The cellular ATP level was markedly decreased in PANC-1 cells grown in nutrient starvation. Mitochondrial inhibitors induced ATP depletion in nutrient-deprived cells at lower concentrations of inhibitors compared with nutrient-sufficient cells, thereby these inhibitors could exert preferential cytotoxicity under nutrient-deprived conditions.

Large areas of tumor are exposed not only to nutrient starvation but also hypoxic conditions. Therefore, we examined preferential cytotoxicity of mitochondrial inhibitors to nutrient-deprived cells in hypoxic conditions. Mitochondrial inhibitors showed preferential cytotoxicity to nutrient-deprived cells not only under hypoxic conditions but also under normoxic conditions. Normal tissue uses glycolysis to generate approximately 10% of the cellular ATP, with mitochondria accounting for 90%. In tumor sections, however, over 50% of the cellular ATP is produced by glycolysis with the remainder being generated at the mitochondria [29]. In hypoxic conditions (1% O_2), HIF-1α was stabilized and accumulated in nutrient-deprived PANC-1 cells, and the real-time PCR analysis revealed that hexokinase 2 and glucose transporter-1 expression were increased (data not shown). Despite PANC-1 cells grown in nutrient-deprived and hypoxic conditions were represented activation of glycolysis and induction of glucose transporter-1, mitochondrial inhibitors exhibited strong cytotoxicity to these cells. Therefore, ATP generation by mitochondria appeared to be essential for cell survival under hypoxic as well as normoxic conditions.

PANC-1 cells are low tumorigenicity even in SCID mice. To examine the *in vivo* antitumor activity of mitochondrial inhibitors, we explored cancer cell lines that were more sensitive to efrapeptin F. The growth inhibitory activity of efrapeptin F against 39 human cancer cell lines of the JFCR39 panel revealed that human prostate cancer PC-3 cells were highly sensitive to efrapeptin F. Thus, PC-3 cancer xenograft models were used to evaluate *in vivo* antitumor activity, and efrapeptin F was found to induce regression of PC-3 xenograft tumors. In this study, we demonstrated that mitochondrial inhibitors showed preferential cytotoxicity to nutrient-deprived cancer cells relative to nutrient-sufficient cells. Therefore, the potent cytotoxicity of these inhibitors to cancer cells deprived of nutrients (simulating a tumor microenvironment) makes mitochondria a promising target for new drugs that may be developed to treat a broad spectrum of malignant tumors.

Acknowledgments

This work was supported by a Grant-in-Aid for the Third-Term Comprehensive 10-Years Strategy for Cancer Control from the Ministry of Health, Labour and Welfare in Japan. We thank Ms. S. Kakuda for technical assistance and the Screening Committee of Anticancer Drugs supported by a Grant-in-Aid for Scientific Research on Priority Area "Cancer" from the Ministry of Education, Culture, Sports, Science and Technology, Japan for supplying the measurement of growth inhibitory activities on 39 human cancer cell lines.

Appendix A. Supplementary data

Supplementary data associated with this article can be found, in the online version, at doi:10.1016/j.bbrc.2010.01.050.

References

[1] P. Vaupel, F. Kallinowski, P. Okunieff, Blood flow, oxygen and nutrient supply, and metabolic microenvironment of human tumors: a review, Cancer Res. 49 (1989) 6449–6465.
[2] J.M. Brown, A.J. Giaccia, The unique physiology of solid tumors: opportunities (and problems) for cancer therapy, Cancer Res. 58 (1998) 1408–1416.
[3] K. Izuishi, K. Kato, T. Ogura, T. Kinoshita, H. Esumi, Remarkable tolerance of tumor cells to nutrient deprivation: possible new biochemical target for cancer therapy, Cancer Res. 60 (2000) 6201–6207.
[4] R. Baserga, The contradictions of the insulin-like growth factor 1 receptor, Oncogene 19 (2000) 5574–5581.
[5] M.N. Pollak, E.S. Schernhammer, S.E. Hankinson, Insulin-like growth factors and neoplasia, Nat. Rev. Cancer 4 (2004) 505–518.
[6] S. Kunimoto, J. Lu, H. Esumi, Y. Yamazaki, N. Kinoshita, Y. Honma, M. Hamada, M. Ohsono, M. Ishizuka, T. Takeuchi, Kigamicins, novel antitumor antibiotics. I. Taxonomy, isolation, physico-chemical properties and biological activities, J. Antibiot. 56 (2003) 1004–1011.
[7] S. Kunimoto, T. Someno, Y. Yamazaki, J. Lu, H. Esumi, H. Naganawa, Kigamicins, novel antitumor antibiotics. II. Structure determination, J. Antibiot. 56 (2003) 1007–1012.
[8] J. Lu, S. Kunimoto, Y. Yamazaki, M. Kaminishi, H. Esumi, H. Esumi, Kigamicin D, a novel anticancer agent based on a new anti-austerity strategy targeting cancer cells' tolerance to nutrient starvation, Cancer Sci. 95 (2004) 547–552.
[9] I. Momose, S. Kunimoto, M. Osono, D. Ikeda, Inhibitors of insulin-like growth factor-1 receptor tyrosine kinase are preferentially cytotoxic to nutrient-deprived pancreatic cancer cells, Biochem. Biophys. Res. Commun. 380 (2009) 171–176.
[10] N.C. Denko, Hypoxia, HIF1 and glucose metabolism in the solid tumour, Nat. Rev. Cancer 8 (2008) 705–723.
[11] R.A. Gatenby, R.J. Gillies, Why do cancers have high aerobic glycolysis?, Nat Rev. Cancer 4 (2004) 891–899.
[12] G. Kroemer, J. Pouyssegur, Tumor cell metabolism: cancer's Achilles' heel, Cancer Cell 13 (2008) 472–482.
[13] A. Hirayama, K. Kami, M. Sugimoto, M. Sugawara, N. Toki, H. Onozuka, T. Kinoshita, N. Saito, A. Ochiai, M. Tomita, H. Esumi, T. Soga, Quantitative metabolome profiling of colon and stomach cancer microenvironment by capillary electrophoresis time-of-flight mass spectrometry, Cancer Res. 69 (2009) 4918–4925.
[14] B. Levine, D.J. Klionsky, Development by self-digestion: molecular mechanisms and biological functions of autophagy, Dev. Cell 6 (2004) 463–477.
[15] S. Gupta, B.S. Krasnoff, W.D. Roberts, A.A.J. Renwick, S.L. Brinen, J. Clardy, Structures of the efrapeptins: potent inhibitors of mitochondrial ATPase from the fungus *Tolypocladium niveum*, J. Am. Chem. Soc. 113 (1991) 707–709.
[16] S. Gupta, B.S. Krasnoff, W.D. Roberts, A.A.J. Renwick, S.L. Brinen, J. Clardy, Structure of efrapeptins from the fungus *Tolypocladium niveum*: peptide inhibitors of mitochondrial ATPase, J. Org. Chem. 57 (1992) 2306–2313.
[17] R.L. Cross, W.E. Kohlbrenner, The mode of inhibition of oxidative phosphorylation by efrapeptin (A23871). Evidence for an alternating site mechanism for ATP synthesis, J. Biol. Chem. 253 (1978) 4865–4873.
[18] M. Kawada, I. Momose, T. Someno, G. Tsujiuchi, D. Ikeda, New atpenins, NBRI23477A and B, inhibit the growth of human prostate cancer cells, J. Antibiot. 62 (2009) 243–246.
[19] T. Mosmann, Rapid colorimetric assay for cellular growth and survival: application to proliferation and cytotoxicity assays, J. Immunol. Methods 65 (1983) 55–63.
[20] M. Ueki, K. Machida, M. Takeuchi, Antifungal inhibitors of mitochondrial respiration: discovery and prospects for development, Curr. Opin. Investig. Drugs 2 (2000) 387–398.
[21] N. Orme-Johnson, Direct and indirect inhibitors of mitochondrial ATP synthesis, Methods Cell Biol. 80 (2007) 813–826.
[22] H. Miyadera, K. Shiomi, H. Ui, Y. Yamaguchi, R. Masuma, H. Tomoda, H. Miyoshi, A. Osanai, K. Kita, S. Omura, Atpenins, potent and specific inhibitors of mitochondrial complex II (succinate-ubiquinone oxidoreductase), Proc. Natl. Acad. Sci. USA 100 (2003) 473–477.
[23] S. Dan, T. Tsunoda, O. Kitahara, R. Yanagawa, H. Zembutsu, T. Katagiri, K. Yamazaki, Y. Nakamura, T. Yamori, An integrated database of chemosensitivity to 55 anticancer drugs and gene expression profiles of 39 human cancer cell lines, Cancer Res. 62 (2002) 1139–1147.
[24] T. Yamori, Panel of human cancer cell lines provides valuable database for drug discovery and bioinformatics, Cancer Chemother. Pharmacol. 52 (Suppl. 1) (2003) S74–S79.
[25] T. Yamori, A. Matsunaga, S. Sato, K. Yamazaki, A. Komi, K. Ishizu, I. Mita, H. Edatsugi, Y. Matsuba, K. Takezawa, O. Nakanishi, H. Kohno, Y. Nakajima, H. Komatsu, T. Andoh, T. Tsuruo, Potent antitumor activity of MS-247, a novel DNA minor groove binder, evaluated by an in vitro and in vivo human cancer cell line panel, Cancer Res. 59 (1999) 4042–4049.
[26] C.V. Dang, G.L. Semenza, Oncogenic alterations of metabolism, Trends Biochem. Sci. 24 (1999) 68–72.
[27] R.M. Southerland, Cell and environment interactions in tumor microregions: the multicell spheroid model, Science 240 (1988) 178–184.
[28] G. Helmlinger, F. Yuan, M. Dellian, R.K. Jain, Interstitial pH and pO_2 gradients in solid tumors in vivo: high-resolution measurements reveal a lack of correlation, Nat. Med. 3 (1997) 177–182.
[29] O. Warburg, On respiratory impairment in cancer cells, Science 124 (1956) 269–270.

UICC
global cancer control

IJC
International Journal of Cancer

Leucinostatin A inhibits prostate cancer growth through reduction of insulin-like growth factor-I expression in prostate stromal cells

Manabu Kawada, Hiroyuki Inoue, Shun-Ichi Ohba, Tohru Masuda, Isao Momose and Daishiro Ikeda

Numazu Bio-Medical Research Institute, Microbial Chemistry Research Center, 18-24 Miyamoto, Numazu-shi, Shizuoka 410-0301, Japan

Fast Track

Targeting stroma in tumor tissues is an attractive new strategy for cancer treatment. We developed *in vitro* coculture system, in which the growth of human prostate cancer DU-145 cells is stimulated by prostate stromal cells (PrSC) through insulin-like growth factor I (IGF-I). Using this system, we have been searching for small molecules that inhibit tumor growth through modulation of tumor-stromal cell interactions. As a result, we have found that leucinostatins and atpenins, natural antifungal antibiotics, inhibit the growth of DU-145 cells cocultured with PrSC more strongly than that of DU-145 cells alone. In this study we examined the antitumor effects of these small molecules *in vitro* and *in vivo*. When DU-145 cells were coinoculated with PrSC subcutaneously in nude mice, leucinostatin A was found to significantly suppress the tumor growth more than atpenin B. The antitumor effect of leucinostatin A *in vivo* was not obtained against the tumors of DU-145 cells alone. RT-PCR experiments revealed that leucinostatin A specifically inhibited IGF-I expression in PrSC without effect on expressions of other IGF axis molecules. Leucinostatins and atpenins are known to abrogate mitochondrial functions. However, when we used mitochondrial DNA-depleted, pseudo-ρ^0 cells, we found that one of leucinostain A actions certainly depended on mitochondrial function, but it actually inhibited the growth of DU-145 cells more strongly in coculture with pseudo-ρ^0 PrSC and reduced IGF-I expression in pseudo-ρ^0 PrSC. Taken together, our results suggested that leucinostatin A inhibited prostate cancer cell growth through reduction of IGF-I expression in PrSC.

Growing evidence indicates that the stroma plays a critical role in the growth and metastasis of various cancers, including colorectal,[1] breast,[2,3] pancreatic[4] and prostate cancer.[5] The constituents of stroma vary in each tissue, but they generally include fibroblasts, macrophages, endothelial cells and extracellular matrix.[6,7] Among these components, certain types of fibroblasts appear to enhance tumor growth and others suppress it.[2,8–10] Fibroblasts that enhance tumor growth are especially referred to as cancer-associated fibroblasts or activated fibroblasts,[11,12] and have distinct characters from normal fibroblasts as they express both vimentin and smooth muscle α-actin (SM α-actin), indicating a myofibroblast phenotype.[6] Theses cells secrete various factors favorable for tumor cell growth, such as growth factors, cytokines and adhesion molecules.[6,12] Thus, tumor-stromal cell interactions can promote tumor growth and metastasis through secreted factors and cell-cell adhesion.[9,10,12,13] Although various kinds of growth factors and cytokines are reported to be involved in tumor-stromal cell interactions, many studies suggest that insulin-like growth factor I (IGF-I) plays an important role in prostate tumor development.[14,15]

The fact that stromal cells can regulate tumor development positively or negatively drives us to consider the modulation of tumor-stromal cell interactions could be an attractive new strategy for the treatment of cancer.[16,17] Some growth factors and antibodies actually suppress the growth of some cancers.[18–20] However, small molecules that modulate tumor-stromal cell interactions are less reported. We therefore constructed an *in vitro* coculture system of prostate cancer cells and PrSC, designed to mimic characteristics of tumors *in vivo*.[14,21] Using this system, we have been searching for small-molecule modulators of tumor-stromal cell interactions. As a result, we found that phthoxazolin A inhibits growth of prostate cancer cells through reduction of IGF-I secretion from PrSC by suppressing myofibroblast differentiation of PrSC.[22]

Moreover, we have recently found that atpenins along with new congeners inhibit growth of prostate cancer cells possibly through modulation of tumor-stromal cell interactions. Further screening has brought about the finding that leucinostatins, fungal metabolites, have great activities in our

Key words: prostate cancer, prostate stroma, natural compound, IGF-I, tumor growth

Additional Supporting Information may be found in the online version of this article.

Grant sponsor: Cancer Research from the Ministry of Education, Culture, Sports, Science, and Technology of Japan

DOI: 10.1002/ijc.24915

History: Received 8 May 2009; Accepted 8 Sep 2009; Online 30 Sep 2009

Correspondence to: Manabu Kawada, Numazu Bio-Medical Research Institute, Microbial Chemistry Research Center, 18-24 Miyamoto, Numazu-shi, Shizuoka 410-0301, Japan, Fax: +81-55-922-6888, E-mail: kawadam@bikaken.or.jp

assay system. In this study, we examined the effects of leucinostatins and atpenins *in vitro* and *in vivo* in respect to modulation of tumor-stromal cell interactions. Here we report that leucinostatin A abrogates tumor-stromal cell interactions through inhibition of IGF-I expression in PrSC and inhibits the growth of prostate cancer cells *in vitro* and *in vivo*.

Material and Methods

Reagents

Rhodanile blue was purchased from Aldrich (Milwaukee, WI). Insulin, hydrocortisone, rotenone, and antimycin A1 were obtained from Sigma (St. Louis, MO). Transferrin was obtained from Wako Pure Chemical Industries (Tokyo, Japan). Recombinant human basic fibroblast growth factor (bFGF) was purchased from Pepro Tech (London, United Kingdom). Antibodies used were anti-IGF-IRβ (sc-713) (Santa Cruz Biotechnology, Santa Cruz, CA) and anti-phosphotyrosine (05-321) (Upstate Biotechnology, Lake Placid, NY). Leucinostatin A and B and atpenin A5 and B were purified from microbial cultured broth in our laboratory.[23]

Cells

The human prostate cancer cell line DU-145 was obtained from the American Type Culture Collection (Manassas, VA) and maintained in Dulbecco's modified Eagle's medium (DMEM) supplemented with 10% fetal bovine serum (FBS; ICN Biomedicals, Aurora, OH), 100 U/ml penicillin G and 100 μg/ml streptomycin at 37°C with 5% CO_2. The human normal prostate stromal cells (PrSC) were obtained from Bio Whittaker (Walkersville, MD) and maintained in DMEM supplemented with 10% FBS, 100 U/ml penicillin G, 100 μg/ml streptomycin, ITH (5 μg/ml insulin, 5 μg/ml transferrin, and 1.4 μM hydrocortisone), and 5 ng/ml bFGF at 37°C with 5% CO_2.

Coculture experiments

A microplate assay method for the selective measurement of epithelial tumor cells in coculture with stromal cells using rhodanile blue dye was performed as previously described.[21] PrSC were first inoculated into 96-well plates at 5,000 cells per well in 100 μl DMEM supplemented with ITH and 0.1% FBS in the presence of various concentrations of test compounds. After 2 days, 10 μl aliquots of DU-145 cell suspension (5,000 cells) in serum-free DMEM were inoculated onto monolayers of PrSC, and the cells were cultured for further 3 days. For monoculture of DU-145 cells, assay medium alone was first incubated in the presence of test compounds for 2 days at 37°C, DU-145 cells were then inoculated as described above, and cultured for further 3 days.

Antitumor effect in vivo

Male or female nude mice, 6-weeks old, were purchased from Charles River Breeding Laboratories (Yokohama, Japan) and maintained in a specific pathogen-free barrier facility according to our institutional guidelines. DU-145 cells (8×10^6) were trypsinized and resuspended with or without PrSC (8×10^6) in 0.3 ml of 10% FBS-DMEM and then combined with 0.5 ml of growth factor-reduced Matrigel (BD Biosciences). One hundred microliters of the cell suspension (1×10^6 cells) were injected subcutaneously in the left lateral flank of mice. Five mice were used for each experimental set. Tumor volume was estimated using the following formula: tumor volume (mm^3) = (length × width^2)/2. After the indicated times, tumors were surgically dissected.

Reverse transcription-PCR and real time PCR analyses

PrSC (2.5×10^5) or DU-145 cells (2.5×10^5) were cultured in DMEM supplemented with ITH and 0.1% FBS in the presence of various concentrations of test compounds for the indicated times. Total RNA was isolated using the RNeasy Minikit (Qiagen, Hilden, Germany). cDNAs were synthesized using avian myeloblastosis virus reverse transcriptase (Promega, Madison, WI) from 1 μg aliquots of RNA and amplified using *Taq* DNA polymerase (Promega). The specific primers used were: cytochrome b (334-bp), 5′-GGCTTACTTCTCTT CATTCTCTCCT-3′ (sense) and 5′- GGTTGTCCTCCAATT CATGTTA-3′ (antisense)[24]; and other primers as reported elsewhere.[14,22] PCR were optimized for each set of primers using different numbers of cycles to ensure that amplification occurred in a linear range. After amplification, products were electrophoresed in 2% agarose gels, stained with SYBR Green I (Cambrex Bio Science, Rockland, ME) and analyzed with a FLA-5000 image analyzer (Fujifilm, Tokyo, Japan). For real time PCR, gene expression was measured in a Thermal Cycler Dice Real Time System (Takara, Shiga, Japan) with SYBR Premix Ex Taq II (Takara).

Preparation of cell lysates and Western blotting

For preparation of PrSC-CM, PrSC (3×10^5) were cultured in DMEM supplemented with 0.1% dialyzed FBS in the presence of various concentrations of test compounds for 2 days. DU-145 cells (5×10^5) were cultured in serum-free DMEM overnight and treated with PrSC-CM for 30 min at 37°C. Cell lysates were prepared and applied to Western blotting with antibodies as previously described.[25]

Preparation of Pseudo-ρ^0 cells

According to the method of Tartier *et al.*,[26] PrSC or DU-145 cells were cultured for 7 days in the presence of 250 ng/ml ethidium bromide in DMEM supplemented with 4.5 mg/ml glucose, 50 μg/ml uridine and 2 mM pyruvate to compensate for the respiratory metabolism deficit.

Statistical analysis

All data are representative of 2 or 3 independent experiments with similar results. Statistical analysis was carried out using Student's *t*-test.

Results

Leucinostatins and atpenins strongly inhibited growth of DU-145 cells in coculture with PrSC

We have been screening for modulators of tumor-stromal cell interactions of prostate cancer cells among natural compounds in microbial cultured broths. We have recently found that atpenins, which were originally reported as antifungal antibiotics and specific inhibitors of mitochondrial complex II,[27–29] inhibited the growth of DU-145 cells in coculture with PrSC more strongly than that of DU-145 cells cultured alone (monoculture) (Fig. 1*b*).[23] Our further screening resulted in the finding of another active microbial cultured broth. We purified the active components and identified them as leucinostatin A and B (Fig. 1*a*). Leucinostatins were originally discovered as antifungal antibiotics.[30–32] As shown in Figure 1*a*, leucinostatins marginally inhibited the growth of DU-145 cells in monoculture, but they strongly inhibited that of DU-145 cells when the cells were cocultured with PrSC. Leucinostatin A did not affect the growth of PrSC (Fig. 1*c*) and leucinostatin B as well as atpenins did not show any cytotoxic effects against PrSC under microscopic observation (data not shown). Rhodanile blue that preferentially stained epithelial cells showed selective decrease in cell numbers of DU-145 cells by leucinostatin A in the coculture with PrSC compared with DU-145 cells alone (Fig. 1*d*). On the other hand, leucinostatin A equally inhibited the growth of NCI-H460 human lung cancer cells in the presence or absence of human lung fibroblasts (Supporting Information Fig. 1). It is suggested that leucinostatin A selectively acts on a particular interaction between tumor and stromal cells.

Leucinostatin A suppressed growth of DU-145 tumors in vivo

Since we obtained rather larger amounts of leucinostatin A and atpenin B compared with the respective analogues, we evaluated the antitumor effects of leucinostatin A and atpenin B *in vivo*. To reflect the result *in vitro*, we inoculated DU-145 cells along with PrSC subcutaneously in nude mice. As a result, leucinostatin A was found to suppress the growth of DU-145 tumors more significantly than atpenin B at lower doses (Fig. 2*a*). Since antitumor effect of leucinostatin A was more potent than atpenin B, we used leucinostatin A mainly for further studies.

Antitumor effect of leucinostatin A depended on coinoculation of PrSC

Because leucinostatin A inhibited the growth of DU-145 cells in coculture with PrSC more strongly than that in monoculture (Fig. 1), we next examined whether the antitumor effect of leucinostatin A depends on the presence of PrSC *in vivo*. As reported previously, coinoculation of PrSC increased the growth of DU-145 tumors (Fig. 2*b*).[14] Leucinostatin A suppressed the growth of DU-145 tumors when the cells were inoculated with PrSC, but it did not affect the growth of DU-145 tumors without PrSC (Fig. 2*b*). This result indicated that leucinostatin A virtually inhibited the additive growth of DU-145 tumors stimulated by coinoculation of PrSC.

Leucinostatin A inhibited IGF-I expression in PrSC

Growing evidence suggests that IGF-I plays a critical role in the development of prostate cancer.[14,15] As we previously reported,[14,33] PrSC are mixtures of fibroblasts and myofibroblasts and IGF-I secreted from PrSC enhances growth of DU-145 cells in the coculture with PrSC (Supporting Information Fig. 2). Furthermore, we have recently reported that phthoxazolin A, another small molecule modulator of tumor-stromal cell interactions, inhibited IGF-I expression in PrSC through suppression of myofibroblast differentiation of PrSC.[22] We therefore examined the effect of leucinostatin A on IGF axis molecules in PrSC. As a result, leucinostatin A was found to specifically inhibit IGF-I expression in PrSC among various IGF axis molecules (Fig. 3*a*). Real time RT-PCR analysis also confirmed that leucinostatin A reduced IGF-I mRNA in PrSC (Fig. 3*b*). Phthoxazolin A inhibits expressions of IGF-1, several IGFBPs, and SM α-actin, a marker of myofibroblast differentiation.[22] However, leucinostatin A failed to inhibit SM α-actin expression and it only slightly inhibited IGFBP-3 expression (Fig. 3*a*).

It is reported that DU-145 cells respond to IGF-I mitogenic signal through IGF-IR.[14] As shown in Figure 3*c* conditioned medium of PrSC increased the phosphorylation of IGF-IR in DU-145 cells due to secreted IGF-I in the conditioned medium.[22] In contrast, conditioned medium prepared from leucinostatin A-treated PrSC actually failed to increase the phosphorylation of IGF-IR in DU-145 cells, indicating the decreased amounts of IGF-I in the conditioned medium of PrSC. Furthermore, leucinostatin A-augmented inhibition of DU-145 cell growth in coculture with PrSC was partially recovered by the external addition of IGF-I (Supporting Information Fig. 3).

Action of leucinostatin A on coculture of DU-145 cells and PrSC was irrespective of mitochondrial function

It is reported that leucinostatins inhibit oxidative phosphorylation in mitochondria.[34] Atpenins are known to be specific inhibitors of mitochondrial complex II.[29] Therefore, we next examined whether the action of leucinostatin A depends on mitochondrial function in cells. We use pseudo-ρ^0 cells that lacked mitochondrial DNA.[26] To verify the status of mitochondrial DNA depletion, we examined the expression of cytochrome b, a component of complex III, which is encoded by mitochondrial DNA.[24] Exposure to ethidium bromide for 7 days resulted in the great reduction of cytochrome b expression in PrSC and DU-145 cells (Fig. 4*a*). Thus, we referred to these cells as pseudo-ρ^0 cells. Among IGF axis molecules IGFBP-3 expression was significantly decreased in pseudo-ρ^0 PrSC. SM α-actin expression was also reduced in

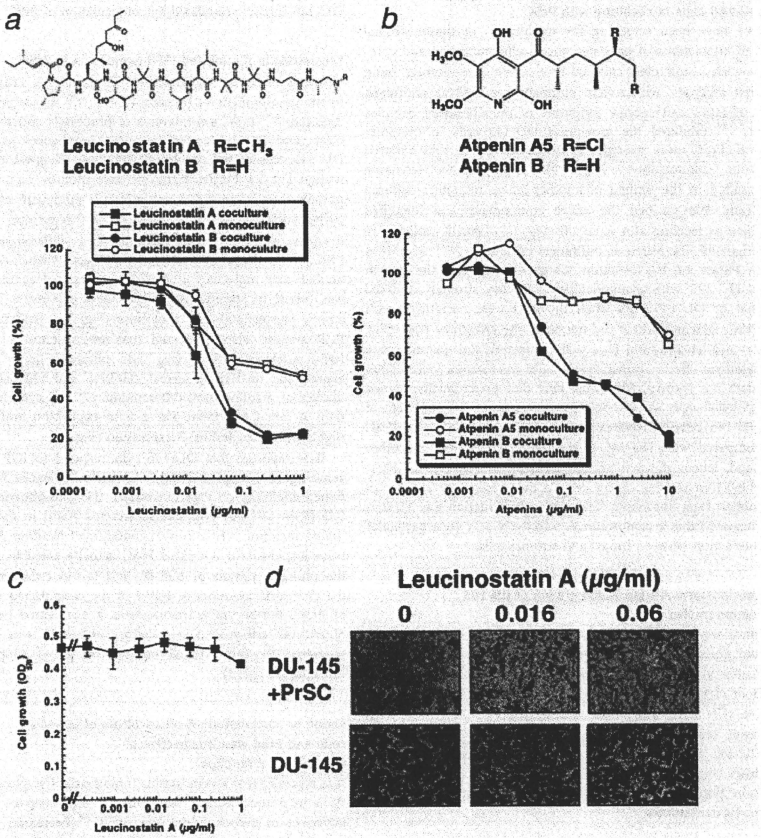

Figure 1. Effect of leucinostatins and atpenins on coculture of DU-145 cells and PrSC. (*a*) Effects of leucinostatin A (squares) and leucinostatin B (circles) on the growth of DU-145 cells alone (open plots) and DU-145 cells cocultured with PrSC (closed plots) were determined using rhodanile blue staining. Values are means ± SD of triplicate determinations. (*b*) Effects of atpenin A5 (circles) and atpenin B (squares) on the growth of DU-145 cells alone (open plots) and DU-145 cells cocultured with PrSC (closed plots) were determined using rhodanile blue staining. Values are means of duplicate determinations [standard errors (SE) less than 10%]. (*c*) Effect of leucinostatin A on the growth of PrSC was determined using MTT. PrSC were cultured alone with the indicated concentrations of leucinostatin A for 2 days. Values are means ± SD of triplicate determinations. (*d*) Representative photos of DU-145 cells cocultured with PrSC and DU-145 cells cultured alone after staining with rhodanile blue. Cells were treated with the indicated concentrations of leucinostatin A. Bar, 200 μm.

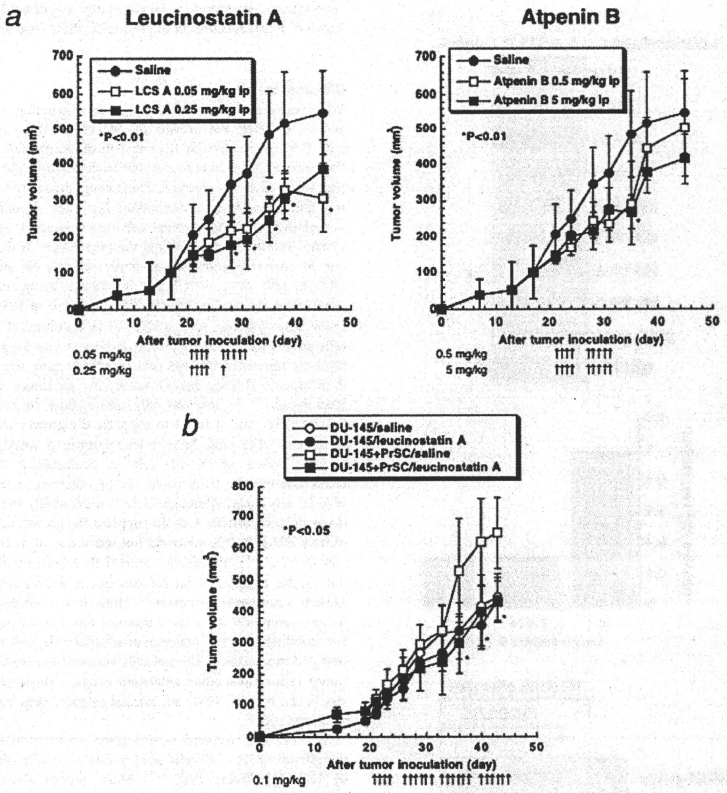

Figure 2. Effects of leucinostatin A and atpenin B on tumor growth of DU-145 cells *in vivo*. (*a*) DU-145 cells were inoculated subcutaneously with PrSC in female nude mice. Leucinostatin A or atpenin B was administered intraperitoneally at the indicated days (arrows). The values are means ± SD of 5 mice. $*p < 0.01$ versus the values with saline. (*b*) DU-145 cells were inoculated subcutaneously with (squares) or without PrSC (circles) in male nude mice. Leucinostatin A at 0.1 mg/kg was administered intraperitoneally at the indicated days (arrows). The values are means ± SD of 5 mice. $*p < 0.05$ versus the values with saline.

pseudo-ρ^0 PrSC suggesting suppression of myofibroblast differentiation, but IGF-I expression was only slightly decreased. Expressions of IGF axis molecules were not affected in pseudo-ρ^0 DU-145 cells. Using these pseudo-ρ^0 cells, we examined the effect of leucinostatin A on coculture of DU-145 cells and PrSC. As a result, leucinostatin A also inhibited the growth of DU-145 cells even cocultured with pseudo-ρ^0 PrSC more strongly than that in monoculture (Fig. 4*c*). In contrast, the growth inhibitory effect of leucinostatin A significantly weakened against pseudo-ρ^0 DU-145 cells suggesting that part of leucinostatin action actually depends on mitochondrial function in DU-145 cells. However, leucinostatin A apparently inhibited the growth of pseudo-ρ^0 DU-145 cells in coculture with PrSC more strongly than that in

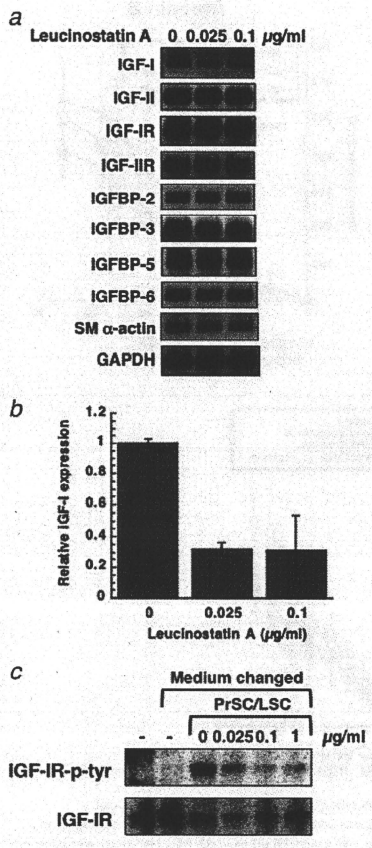

Figure 3. Effect of leucinostatin A on expression of IGF axis molecules in PrSC. (*a*) PrSC were cultured with leucinostatin A for 2 days. Total RNAs were collected and RT-PCR for the indicated molecules was carried out using specific primers. (*b*) IGF-I mRNA levels were analyzed by real time RT-PCR using GAPDH as a reference. (*c*) Conditioned medium was prepared from PrSC cultured with the indicated concentrations of leucinostatin A for 2 days (PrSC/LSC). DU-145 cells were treated with the conditioned medium or normal medium for 30 min (Medium changed). Cell lysates were prepared and applied to immunoprecipitation of IGF-IR for the detection of tyrosine-phosphorylated IGF-IR and total IGF-IR.

monoculture. Furthermore, leucinostatin A specifically inhibited IGF-I expression even in pseudo-ρ^0 PrSC (Fig. 4*b*).

Discussion

We have recently reported that atpenins including new congeners inhibited the growth of DU-145 cells in coculture with PrSC more strongly than that in monoculture.[23] By further screening, we have found that leucinostatins also showed the same activity as atpenins. These compounds are originally reported as antifungal antibiotics, but they should act as modulators of tumor-stromal cell interactions in our assay system. We therefore examined the possibilities in this study. For *in vivo* evaluation of antitumor activity, we inoculated DU-145 cells along with PrSC subcutaneously, because DU-145 tumors were stimulated by coinoculation of PrSC[14] and the screening system was carried out as coculture of DU-145 cells and PrSC. As a result, leucinostatin A was found to inhibit the tumors of DU-145 cells and PrSC more significantly than atpenin B (Fig. 2*a*). However, the antitumor effect of leucinostatin A *in vivo* was only seen against the coinoculation of PrSC, and it failed to suppress the growth of tumors of only DU-145 cells. *In vitro* leucinostatin A weakly inhibited the growth of DU-145 cells in monoculture, but such direct antitumor activity could not be obtained in the doses used in this study. Although there is a possibility that higher doses of leucinostatin A could suppress the growth of tumors of only DU-145 cells, we could not test it due to its high toxicity in mice. It is previously reported that leucinostatins cannot inhibit Ehrlich ascites tumors, but it weakly suppresses Ehrlich subcutaneous tumors.[30] Thus, it is considered that leucinostatins will show the antitumor effect *in vivo* in a certain condition such as presence of stromal cells. It is reported that p53 mutations in stromal cells augment the sensitivity of tumor cells against some antitumor drugs.[35] However, this is less likely, because PrSC are normal primary cells harboring wild type p53.[36]

DU-145 cells respond to mitogenic action of IGF-I, and the growth of DU-145 cells *in vitro* and *in vivo* is stimulated by IGF-I producing PrSC.[14,33] Many reports showed that IGF-I is one of critical mediators of tumor-stromal cell interactions in prostate.[15] Thus, there is a high possibility that active compounds in our assay system act on the IGF-I signals. In fact, we have recently reported that phthoxazolin A, another active compound in our assay system, inhibited the IGF-I expression in PrSC through suppression of myofibroblast differentiation of PrSC.[22] Although the real contribution of SM α-actin positive myofibroblasts to the tumor promotion is still controversial, the production of IGF-I in stromal cells is critical for growth of some tumors. Therefore, in respect to the mechanism of leucinostatin action we focused on IGF-I axis. As a result, we have found that leucinostatin A specifically inhibited IGF-I expression in PrSC (Fig. 3). Because phthoxazolin A also inhibited expressions of various IGFBPs and SM α-actin in addition to IGF-I, the mechanism

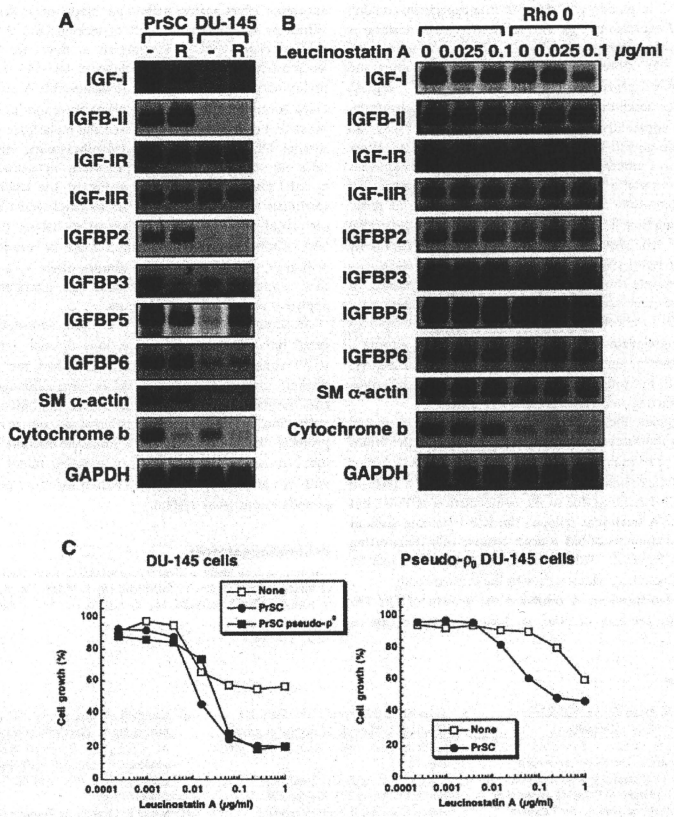

Figure 4. Effect of leucinostatin A on pseudo-ρ^0 cells. (*a*) PrSC and DU-145 cells were cultured with (R) or without (-) ethidium bromide. Total RNAs were collected and RT-PCR for the indicated molecules was carried out using specific primers. (*b*) PrSC or pseudo-ρ^0 PrSC (Rho0) were cultured with leucinostatin A for 2 days. Total RNAs were collected and RT-PCR for the indicated molecules was carried out using specific primers. (*c*) Effect of leucinostatin A on the growth of DU-145 cells (left) or pseudo-ρ^0 DU-145 cells (right) alone (open squares) or cocultured with PrSC (closed circles) or pseudo-ρ^0 PrSC (closed squares) was determined using rhodanile blue staining. Values are means of triplicate determinations [standard errors (SE) less than 10%].

of lecinostatins action was considered to be different from that of phthoxazolin A.

Leucinostatins are reported to inhibit oxidative phosphorylation in mitochondria[34] and atpenins are known as inhibitors of mitochondrial complex II.[29] There is a possibility that abrogation of mitochondrial functions could involve in the activity in our assay system. To examine the possible involvement of mitochondrial function in our assay system we employed pseudo-ρ^0 cells. Abrogation of mitochondrial functions resulted in reduction of the expression of SM α-actin

and IGFBP-3 in pseudo-ρ^0 PrSC, but it unexpectedly couldn't affect IGF-I expression (Fig. 4). Furthermore, leucinostatin A inhibited the growth of DU-145 cells cocultured with pseudo-ρ^0 PrSC more strongly than that in monoculture and decreased IGF-I expression even in pseudo-ρ^0 PrSC (Fig. 4). On the other hand, the growth inhibitory effect of leucinostatin A was apparently weakened against pseudo-ρ^0 DU-145 cells, but the growth of pseudo-ρ^0 DU-145 cells in coculture with PrSC was inhibited more strongly than that in monoculture by leucinostatin A (Fig. 4). These results indicated that one of leucinostatin action was actually inhibition of mitochondrial function. This result correlated well with the partial recovery of leucinostatin A-inuduced growth inhibition by the external IGF-I (Supporting Information Fig. 3). However, there is certainly another mechanism for the inhibition of IGF-I expression, which brought about the inhibition of growth of DU-145 cells in coculture with PrSC. It is reported that c-jun upregulates IGF-I production in prostate stroma.[37] We examined the effect of leucinostatin A on c-jun expression in PrSC, but found no change in response to leucinostatin A (Supporting Information Fig. 3).

To extrapolate the *in vitro* finding to *in vivo*, we examined whether leucinostatin A reduces IGF-I expression in the tumor tissues. Our preliminary results revealed that DU-145 tumor tissues contained significant amounts of SM α-actin positive cells and IGF-I staining due to the coinoculation of PrSC, but leucinostatin A treatment reduced the IGF-I staining without effect on the amounts of SM α-actin positive cells (Supporting Information Figure 4). Although more precise studies must be needed, this result correlates well with the *in vitro* result.

Because leucinostatin A inhibited the growth of DU-145 tumors in the presence of PrSC, we have tried to evaluate its antitumor effect against orthotopic model of prostate tumors. When we examined the effect of leucinostatin A on orthotopic implanted DU-145 xenograft in mice, we found that leucinostatin A inhibited metastases of DU-145 tumors. Our preliminary results showed that leucinostatin A unfortunately failed to inhibit the growth of primary tumors in the mouse prostate, but it possibly suppressed the metastases of DU-145 tumors. DU-145 tumors formed diaphragmatic metastases (4 mice out of 6 mice, 67%) and peritoneal metastases (5 out of 6, 83%) (Supporting Information Fig. 5), but leucinostatin A treatment reduced the metastases as diaphragmatic metastases (1 out of 3, 33%) and peritoneal metastases (0 out of 3, 0%). Although further evaluation must be needed for the orthotopic model of prostate tumors, there is a possibility that modulators of tumor-stromal cell interactions could apply for antimetastases of tumors.

In summary our results showed that leucinostatin A abrogated tumor-stromal cell interactions through inhibition of IGF-I expression from PrSC and inhibited the growth of prostate cancer cells *in vitro* and *in vivo*. Although the precise mechanism of leucinostatin A on inhibition of IGF-I expression in PrSC is needed further study, our results clearly promote the notion that small molecule modulators of tumor-stromal cell interactions can suppress tumor growth *in vivo*. We are now continuing to search for more potent compounds in our assay system.

Acknowledgements

The authors are grateful to Meiji Seika Kaisha, Ltd. for fermentation broths of fungal strains and Dr. Y. Takahashi, Dr. T. Shitara, Ms. I. Kurata, Dr. T. Someno, Dr. M. Arakawa, Ms. K. Adachi, and Ms. E. Satoh for their technical assistance.

References

1. Stahtea XN, Roussidis AE, Kanakis I, Tzanakakis GN, Chalkiadakis G, Mavroudis D, Kletsas D, Karamanos NK. Imatinib inhibits colorectal cancer cell growth and suppresses stromal-induced growth stimulation. MT1-MMP expression and pro-MMP2 activation. *Int J Cancer* 2007;121:2808–14.
2. Wiseman BS, Werb Z. Stromal effects on mammary gland development and breast cancer. *Science* 2002;296:1046–9.
3. Karnoub AE, Dash AB, Vo AP, Sullivan A, Brooks MW, Bell GW, Richardson AL, Polyak K, Tubo R, Weinberg RA. Mesenchymal stem cells within tumour stroma promote breast cancer metastasis. *Nature* 2007;449:557–63.
4. Hwang RF, Moore T, Arumugam T, Ramachandran V, Amos KD, Rivera A, Ji B, Evans DB, Logsdon CD. Cancer-associated stromal fibroblasts promote pancreatic tumor progression. *Cancer Res* 2008;68:918–26.
5. Grossfeld GD, Hayward SW, Tlsty TD, Cunha GR. The role of stroma in prostatic carcinogenesis. *Endocr Relat Cancer* 1998;5: 253–70.
6. Tuxhorn JA, Ayala GE, Smith MJ, Smith VC, Dang TD, Rowley DR. Reactive stroma in human prostate cancer: induction of myofibroblast phenotype and extracellular matrix remodeling. *Clin Cancer Res* 2002;8: 2912–23.
7. Dvorak HF. Tumors: wounds that do not heal. Similarities between tumor stroma generation and wound healing. *N Engl J Med* 1986;315:1650–9.
8. Delinassios JG. Cytocidal effects of human fibroblasts on HeLa cells in vitro. *Biol Cell* 1987;59:69–77.
9. Picard O, Rolland Y, Poupon MF. Fibroblast-dependent tumorigenicity of cells in nude mice: implication for implantation of metastases. *Cancer Res* 1986;46:3290–4.
10. Camps JL, Chang SM, Hsu TC, Freeman MR, Hong SJ, Zhau HE, von Eschenbach AC, Chung LW. Fibroblast-mediated acceleration of human epithelial tumor growth *in vivo*. *Proc Natl Acad Sci USA* 1990;87:75–9.
11. Micke P, Ostman A. Tumour-stroma interaction: cancer-associated fibroblasts as novel targets in anti-cancer therapy? *Lung Cancer* 2004;45 (Suppl 2):S163–S175.
12. Tuxhorn JA, Ayala GE, Rowley DR. Reactive stroma in prostate cancer progression. *J Urol* 2001;166:2472–83.
13. Wernert N. The multiple roles of tumour stroma. *Virchows Arch* 1997;430:433–43.
14. Kawada M, Inoue H, Masuda T, Ikeda D. Insulin-like growth factor I secreted from prostate stromal cells mediates tumor-stromal cell interactions of prostate cancer. *Cancer Res* 2006;66:4419–25.
15. Pollak M, Beamer W, Zhang JC. Insulin-like growth factors and prostate cancer. *Cancer Metastasis Rev* 1998;17:383–90.

16. Kiaris H, Trimis G, Papavassiliou AG. Regulation of tumor-stromal fibroblast interactions: implications in anticancer therapy. *Curr Med Chem* 2008;15: 3062–7.
17. Tsellou E, Kiaris H. Fibroblast independency in tumors: implications in cancer therapy. *Future Oncol* 2008;4: 427–32.
18. Date K, Matsumoto K, Kuba K, Shimura H, Tanaka M, Nakamura T. Inhibition of tumor growth and invasion by a four-kringle antagonist (HGF/NK4) for hepatocyte growth factor. *Oncogene* 1998; 17:3045–54.
19. Kawada M, Ishizuka M, Takeuchi T. Enhancement of antiproliferative effects of interleukin-1β and tumor necrosis factor-α on human prostate cancer LNCaP cells by coculture with normal fibroblasts through secreted interleukin-6. *Jpn J Cancer Res* 1999;90:546–54.
20. Tuxhorn JA, McAlhany SJ, Yang F, Dang TD, Rowley DR. Inhibition of transforming growth factor-β activity decreases angiogenesis in a human prostate cancer-reactive stroma xenograft model. *Cancer Res* 2002;62:6021–5.
21. Kawada M, Yoshimoto Y, Minamiguchi K, Kumagai H, Someno T, Masuda T, Ishizuka M, Ikeda D. A microplate assay for selective measurement of growth of epithelial tumor cells in direct coculture with stromal cells. *Anticancer Res* 2004;24: 1561–8.
22. Kawada M, Inoue H, Usami I, Ikeda D. Phthoxazolin A inhibits prostate cancer growth by modulating tumor-stromal cell interactions. *Cancer Sci* 2009;100:150–7.
23. Kawada M, Momose I, Someno T, Tsujiuchi G, Ikeda D. New atpenins, NBRI23477 A and B, inhibit the growth of human prostate cancer cells. *J Antibiot* 2009;62:243–6.
24. Kent RJ, Norris DE. Identification of mammalian blood meals in mosquitoes by a multiplexed polymerase chain reaction targeting cytochrome B. *Am J Trop Med Hyg* 2005;73:336–42.
25. Kawada M, Masuda T, Ishizuka M, Takeuchi T. 15-Deoxyspergualin inhibits Akt kinase activation and phosphatidylcholine synthesis. *J Biol Chem* 2002;277:27765–71.
26. Tartier L, Gilchrist S, Burdak-Rothkamm S, Folkard M, Prise KM. Cytoplasmic irradiation induces mitochondrial-dependent 53BP1 protein relocalization in irradiated and bystander cells. *Cancer Res* 2007;67:5872–9.
27. Omura S, Tomoda H, Kimura K, Zhen DZ, Kumagai H, Igarashi K, Imamura N, Takahashi Y, Tanaka Y, Iwai Y. Atpenins, new antifungal antibiotics produced by *Penicillium sp.* Production, isolation, physico-chemical and biological properties. *J Antibiot* 1988;41:1769–73.
28. Kumagai H, Nishida H, Imamura N, Tomoda H, Omura S, Bordner J. The structures of atpenins A4. A5 and. B, new antifungal antibiotics produced by *Penicillium sp. J Antibiot.* 1990;43:1553–8.
29. Miyadera H, Shiomi K, Ui H, Yamaguchi Y, Masuma R, Tomoda H, Miyoshi H, Osanai A, Kita K, Omura S. Atpenins, potent and specific inhibitors of mitochondrial complex II (succinate-ubiquinone oxidoreductase). *Proc Natl Acad Sci USA* 2003;100:473–7.
30. Arai T, Mikami Y, Fukushima K, Utsumi T, Yazawa K. A new antibiotic, leucinostatin, derived from *Penicillium lilacinum.*. *J Antibiot* 1973;26:157–61.
31. Fukushima K, Arai T, Mori Y, Tsuboi M, Suzuki M. Studies on peptide antibiotics, leucinostatins. I. Separation, physico-chemical properties and biological activities of leucinostatins A and B. *J Antibiot* 1983; 36:1606–12.
32. Fukushima K, Arai T, Mori Y, Tsuboi M, Suzuki M. Studies on peptide antibiotics, leucinostatins. II. The structures of leucinostatins A and B. *J Antibiot* 1983;36: 1613–30.
33. Kawada M, Inoue H, Arakawa M, Ikeda D. Transforming growth factor-β1 modulates tumor-stromal cell interactions of prostate cancer through insulin-like growth factor-I. *Anticancer Res* 2008;28:721–30.
34. Shima A, Fukushima K, Arai T, Terada H. Dual inhibitory effects of the peptide antibiotics leucinostatins on oxidative phosphorylation in mitochondria. *Cell Struct Funct* 1990;15:53–8.
35. Lafkas D, Trimis G, Papavassiliou AG, Kiaris H. P53 mutations in stromal fibroblasts sensitize tumors against chemotherapy. *Int J Cancer* 2008;123: 967–71.
36. Bromfield GP, Meng A, Warde P, Bristow RG. Cell death in irradiated prostate epithelial cells: role of apoptotic and clonogenic cell kill. *Prostate Cancer Prostatic Dis* 2003;6:73–85.
37. Li W, Wu CL, Febbo PG, Olumi AF. Stromally expressed c-Jun regulates proliferation of prostate epithelial cells. *Am J Pathol* 2007;171:1189–98.

Fast Track

Biosci. Biotechnol. Biochem., **74** (9), 1913–1919, 2010

Increased ABCB1 Expression in TP-110-Resistant RPMI-8226 Cells

Masatomi IIJIMA,† Isao MOMOSE, and Daishiro IKEDA

Numazu Bio-Medical Research Institute, Microbial Chemistry Research Center, 18-24 Miyamoto, Numazu, Shizuoka 410-0301, Japan

Received April 27, 2010; Accepted June 11, 2010; Online Publication, September 7, 2010
[doi:10.1271/bbb.100325]

TP-110, a novel proteasome inhibitor, has been found to possess potent growth inhibition in human multiple myeloma cells. To enhance its therapeutic effects, we established TP-110-resistant RPMI-8226 (RPMI-8226/TP-110) cells and elucidated their resistance mechanisms. The IC_{50} value for TP-110 cytotoxicity in the RPMI-8226/TP-110 cells was about 10-fold higher than that of the parental sensitive cells. The RPMI-8226/TP-110 cells exhibited distinct drug resistance to other proteasome inhibitors. Furthermore, they showed high cross-resistance to the cytotoxic effects of doxorubicin, etoposide, taxol, and vincristine. P-glycoprotein (MDR1), encoded by *ABCB1*, was elevated in the RPMI-8226/TP-110 cells, and the MDR1 inhibitor verapamil overcame their resistance to TP-110. The results of DNA microarray and RT-PCR suggested that the expression of ABCB1 is significantly elevated in RPMI-8226/TP-110 cells. This indicates that resistance in RPMI-8226/TP-110 cells is involved in the expression of P-glycoprotein, a drug-efflux pump.

Key words: proteasome inhibitor; ABCB1; TP-110

The ubiquitin-proteasome system is involved in the cell cycle, signal transduction, the cellular stress response, and the immune response.[1] Because cancer cells are more highly proliferative than normal cells, their protein translation and degradation is also higher.[2] Accordingly, inhibitors of the proteasome represent a promising group of chemotherapeutic agents for cancer treatment.

Previous research has demonstrated that MG-132, lactacystin, and bortezomib have proteasome inhibitory activities.[3–5] Bortezomib, a dipeptide boronic acid, shows significant anti-tumor activity in multiple myeloma cells. In 2003, the U.S. Food and Drug Administration (FDA) approved bortezomib (VELCADE™), formerly known as PS-341, for the treatment of relapsed/refractory multiple myeloma.[6]

We have reported the isolation of a new proteasome inhibitor, tyropeptin A, produced by *Kitasatospora* sp. MK993-dF2.[7–10] In an effort to enhance its inhibitory potency, a structural model of tyropeptin A bound to the site responsible for chymotrypsin-like activity of the mammalian 20S proteasome was constructed. Based on these modeling experiments, several derivatives were synthesized. One of them, TP-110, specifically inhibits chymotrypsin-like activity, but does not inhibit the post-glutamyl-peptide hydrolyzing (PGPH) and trypsin-like activities of the 20S proteasome.[11] TP-110 strongly inhibits the growth of human tumor cells and induces apoptosis.[12] One of the mechanisms of apoptosis induction by TP-110 is down-regulation of inhibitors of apoptosis proteins (IAPs) in multiple myeloma cells.[13]

A loss of anti-tumor efficacy responsible for drug-resistance in cells is known in cancer chemotherapy. ABC (ATP binding cassette) transporters are well-known multi-drug efflux transporters that depend on ATP.[14] One of these, ABCB1 (MDR1), is a representative transporter involved in human multi-drug resistant tumor cells. In addition to ABCB1, expression of ABCC1 (MRP1) and ABCG2 (BCRP) has also been found in tumor cell lines.[15–17] To overcome multi-drug resistance (MDR), MDR inhibitors have been developed. Verapamil, cyclosporin A and tamoxifen are first-generation MDR inhibitors,[18] and the next generation of inhibitors and antibodies for MDR are now being studied.[19] These inhibitors or antibodies might significantly contribute to overcoming anticancer drug resistance.

We have been developing novel proteasome inhibitors as candidate anti-tumor agents. To strengthen their therapeutic effects, we have also been investigating methods of overcoming resistance. Here we report the involvement of ABCB1 in the resistance mechanisms of RPMI-8226/TP-110 cells.

Materials and Methods

Chemicals and antibodies. TP-110, a tyropeptin A derivative, was synthesized at the Numazu Bio-Medical Research Institute, Numazu, Japan.[9] It was dissolved in DMSO (10 mg/ml), stored at −20 °C, and diluted with PBS (pH 7.4). The chemical structure of TP-110 is shown in Fig. 1. MG-132 and lactacystin were purchased from the Peptide Institute (Osaka, Japan). Bortezomib was synthesized at the Microbial Chemistry Research Institute (Tokyo, Japan). Anti-cancer drugs were purchased from Sigma (St. Louis, MO). Antibodies were obtained as follows: rabbit anti-caspase-3 (sc-7148) and rabbit anti-mdr (sc-8313) (Santa Cruz Biotechnology, Santa Cruz, CA); mouse anti-cytochrome *c* (7H8.2C12) (BD BioScience, San Diego); mouse anti-α-tubulin (B-5-1-2) (Sigma); and mouse anti-mrp1 (QCRL-1) (Chemicon International, Temecula, CA).

Cells and establishment of TP-110-resistant cells. Human multiple myeloma RPMI-8226 cells were purchased from ATCC. Initial induction of resistant cells were achieved by continuous exposure of RPMI-8226 cells to TP-110 (10 ng/ml) over 3 months. Growing resistant cells were further treated with gradually increasing concen-

† To whom correspondence should be addressed. Fax: +81-55-922-6888; E-mail: iijimam@bikaken.or.jp
Abbreviations: ABC, ATP binding cassette; MDR, multidrug resistance; P-gp, P-glycoprotein; IAPs, intrinsic inhibitor of apoptosis proteins

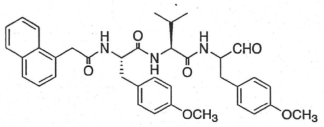

Fig. 1. Structure of TP-110.

trations of TP-110 (up to a final concentration of 100 ng/ml for RPMI-8226 cells). The resistant RPMI-8226 cells that survived exposure to TP-110 (100 ng/ml) were cloned by the limiting dilution method. Chronic leukemia K-562 cells and doxorubicin-resistant K-562 (K-562/DOX) cells were provided by Dr. Setsuko Kunimoto at our laboratory. Cells were grown in RPMI1640 medium supplemented with 10% FBS, 100 U/ml of penicillin G, and 100 μg/ml of streptomycin at 37 °C with 5% CO_2.

Proteasome activity. The chymotrypsin-like activity of the 20S proteasome was measured using a fluorogenic substance, as described previously.[7] The 20S proteasome was prepared from RPMI-8226 and RPMI-8226/TP-110 cells.

Cytotoxicity. Cells (1×10^4) were cultured in 96-well plates with a test sample. Cells from 72 h culture were pulsed with MTT (3-(4,5-dimethyl-2-thiazolyl)-2,5-diphenyl-2H-tetrazolium bromide) for 4 h, and were incubated in the presence of 10% SDS for 20 h. Absorbance was measured at 570 nm using a spectrophotometer (Dainippon Sumitomo Pharma, Osaka, Japan).

Cell cycle analysis. Cells (1×10^4) were cultured with and without 0.1 μg/ml TP-110 for 24 h. Cells fixed using 70% ethanol were treated with 0.1% RNase A at 37 °C for 15 min, and were then incubated with propidium iodide (PI). DNA fluorescence was analyzed using a fluorescence-activated cell sorter (FACSCalibur; BD Bioscience, Franklin Lakes, NJ).

Caspase-3 activity. Cells (5×10^5) were cultured with TP-110 for 24 h, washed twice with PBS, and lysed in cell extraction buffer containing 50 mM HEPES (pH 7.4), 5 mM CHAPS, and 5 mM DTT, and were stored at −80 °C. Cell extracts were centrifuged at 14,000 × *g* for 10 min at 4 °C, and the caspase-3 activity of the supernatant was assessed with a caspase-3 assay kit (Sigma). This assay is based on the hydrolysis of a peptide substrate, acetyl-Asp-Glu-Val-Asp-7-amino-4-methylcoumarin (Ac-DEVD-AMC), by caspase-3. After incubation at 37 °C for 30 min, fluorescence intensity (excitation and emission wavelengths of Ac-DEVD-AMC, 380 nm and 460 nm respectively) was measured with Fluoroskan II (Dainippon Sumitomo Pharma, Osaka, Japan).

Western blot analysis. Cultured cells were harvested, washed twice with PBS, and suspended in lysis buffer containing 20 mM HEPES (pH 7.5), 150 mM NaCl, 1% Triton X-100, 10% glycerol, 1 mM EDTA, 50 mM NaF, 50 mM β-glycerophosphate, 1 mM Na_3VO_4, 25 μg/ml of antipain, 25 μg/ml of leupeptin and 25 μg/ml of pepstatin at 4 °C for 15 min. After centrifugation at 15,000 rpm, the supernatant was assessed using a Bio-Rad protein assay kit (Bio-Rad, Hercules, CA). The cytosol fraction was extracted at 4 °C for 5 min using digitonin lysis buffer containing 10 mM HEPES, 0.3 M mannitol 0.1% BSA, and 0.1 mM digitonin, and centrifuged at 8,500 × *g* for 5 min at 4 °C. Equal amounts of the protein extract were subjected to SDS–PAGE. The isolated protein was then transferred onto an Immobion PVDF membrane (Millipore, Bedford, MA). The membrane was blocked with 5% non-fat milk in Tris-buffered saline containing 0.1% Tween 20 (TBS-T) for 60 min. After washing with TBS-T, the membrane was incubated with primary antibody in blocking solution for 60 min at room temperature. After further washing with TBS-T, the membrane was then incubated with secondary antibody (anti-rabbit or anti-mouse immunoglobulin-horseradish peroxidase) for 30 min. The protein detected was visualized by the enhanced chemiluminescence reaction (ECL) procedure (GE Healthcare UK, Chalfont, UK).

Table 1. Growth Inhibitory Activity of TP-110 on Established Clones of RPMI-8226 Cells

		IC_{50} (μg/ml)	Index of resistance
RPMI-8226		0.020	1
RPMI-8226/TP-110	Clone 1	0.26	13
	Clone 2	0.18	9
	Clone 3	0.40	20
	Clone 4	0.31	16
	Clone 5	0.39	20
	Clone 6	0.45	23
	Clone 7	0.46	23
	Clone 8	0.47	24
	Clone 9	0.43	22
	Clone 10	0.25	13

RT-PCR analysis. Total RNA was isolated from the cells using an RNeasy Kit (Qiagen, Valencia, CA). cDNA was prepared from total RNA using a Reverse Transcription System (Promega, Madison, WI). PCR was conducted using Promega PCR Master Mix (Promega) and a pair of specific primers. The primers used were as follows: *ABCB1*-sense 5′-AGAGGATCGCCATTGCGCGT-3′ and *ABCB1*-antisense 5′-CCTGCTGTCTGCATTGTGAC-3′; *ABCC1*-sense AGTGACCTC-TGGTCCTTAAACAAGG-3′ and *ABCC1*-antisense GAGGTAGAG-AGCAAGGTAGACTTGC-3′; and *GAPDH*-sense 5′-GATGACATC-AAGAAGGTGGTGAA-3′ and *GAPDH*-antisense 5′-GTCTTACTCC-TTGGAGGCCTAGT-3′. The PCR products were electrophoresed on 2% agarose gels, and were detected by SYBR Green I nucleic acid gel staining (Molecular Probes, Eugene, OR).

cDNA microarray analysis. Labeled antisense RNA was prepared from the total RNA of the cells using of an RNA Transcript Sure LABEL Core Kit (Takara Bio, Ohtsu, Japan) with Cy3- and Cy5-dUTP (GE Healthcare, Piscataway, NJ). The cDNA microarray system used the IntelliGene HS Human Expression CHIP, which contains 16,600 spots of cDNA sequences. Microarrays were scanned using a 428-Array Scanner (Affymetrix, Santa Clara, CA).

Results

Establishment of RPMI-8226/TP-110 cells

RPMI-8226/TP-110 cells were developed over a 9-month period by continuous stepwise exposure to increasing concentrations of TP-110, and 10 clones were isolated by the limiting dilution method. The IC_{50} value for TP-110 cytotoxicity in the RPMI-8226/TP-110 cells showed a 9 to 24-fold increase as compared to the parental sensitive cells. Among these, we selected three strains (clone 2, clone 5, and clone 7), that exhibited distinct indices of resistance (Table 1).

Characteristics of the RPMI-8226/TP-110 cells

The morphology of RPMI-8226/TP-110 cells did not change as compared to the parent cells. Although the endogenous proteasome activities of RPMI-8226/TP-110 increased 1.4 to 1.6 fold, the sensitivity of the proteasome to TP-110 in the RPMI-8226/TP-110 cells were similar to that of the parent cells (Fig. 2A and B). Previous studies have indicated that TP-110 induced apoptosis in RPMI-8226 cells at 12 nM.[11] The effects of TP-110 on the cell cycle of the parent and the resistant cells are shown in Fig. 3A. Treatment with TP-110 for 24 h increased the number of cells in sub-G_1 and decreased the number of cells in G_1 and G_2M on the parent sensitive cells. However, the RPMI-8226/TP-110 cells were tolerant of TP-110 (Fig. 3A). Similarly, the

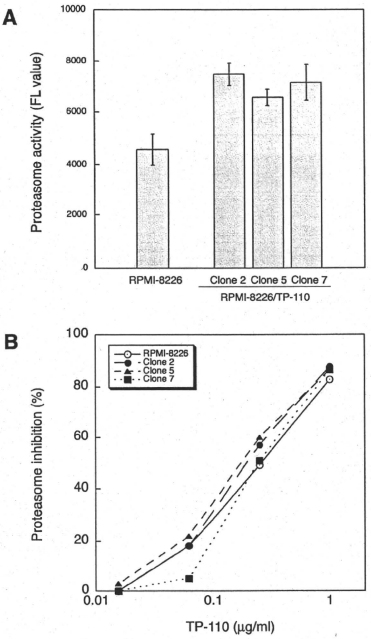

Fig. 2. Proteasome Activity in RPMI-8226/TP-110 Cells.
A, Protein extracts from 1×10^5 cells were assessed. The chymotrypsin-like activity of 20S proteasome was measured as described in "Materials and Methods." B, Inhibition of 20S proteasome by TP-110 in established resistant cells. TP-110 was added to the various enzyme reaction mixture.

addition of TP-110 to the parent sensitive cells strongly released cytochrome *c* into the cytosol, induced the active form of caspase-3, and increased caspase-3 activity, but the addition of TP-110 to RPMI-8226/TP-110 cells did not produce similar results (Fig. 3B, C, and D). This suggests that RPMI-8226/TP-110 cells are tolerant TP-110.

Cross-resistance pattern of RPMI-8226/TP-110 cells

Drug-resistant cells often exhibit cross-resistance to other drugs. First, we examined the cross-resistance to other proteasome inhibitors of RPMI-8226/TP-110 cells. The RPMI-8226/TP-110 cells showed cross-resistance to MG-132 (2.9 to 3.5 fold) and bortezomib (1.4 to 2.1 fold), but these cells showed no cross-resistance to lactacystin. Second, the cross-resistance to several anticancer drugs of RPMI-8226/TP-110 cells was examined. The RPMI-8226/TP-110 cells were also cross-resistant to DNA-interacting drugs, mitosis blocking drugs, topo II inhibitors, and anti-metabolite drugs. In particular, they showed potent cross-resistance to doxorubicin (40 to 115 fold), taxol (375 to 500 fold), vincristine (212 to 253 fold), and etoposide (202 to 396 fold) (Table 2).

Table 2. Cytotoxic Effects of Proteasome Inhibitors and Antitumor Agents on RPMI-8226/TP-110 Cells

Compound	IC_{50} (μg/ml)			
	RPMI-8226	RPMI-8226/TP-110		
		Clone 2	Clone 5	Clone 7
TP-110	0.030	0.37 (12*)	0.34 (11)	0.21 (7.0)
MG-132	0.48	1.4 (2.9)	1.7 (3.5)	1.6 (3.3)
Bortezomib	0.0018	0.0025 (1.4)	0.0037 (2.1)	0.0031 (1.7)
Lactacystin	1.0	0.71 (0.70)	0.53 (0.53)	0.76 (0.76)
Doxorubicin	0.0080	0.32 (40)	0.92 (115)	0.84 (114)
Mitomycin C	0.16	0.42 (2.6)	0.54 (3.4)	0.77 (4.8)
Actinomycin D	0.0074	0.18 (24)	0.33 (44)	0.45 (61)
Taxol	0.0080	3.1 (388)	4.0 (500)	3.0 (375)
Vincristine	0.0017	0.43 (253)	0.36 (212)	0.42 (247)
Vinblastine	0.0078	0.17 (22)	0.14 (18)	0.19 (24)
Etoposide	0.048	9.7 (202)	19 (396)	17 (354)
5-Fluorouracil	0.24	0.66 (2.8)	0.17 (0.71)	0.44 (1.8)

*Values in parentheses indicate index of resistance (fold).

DNA microarray analysis

DNA microarray analysis is informative in elucidating the mechanisms of drug action. Parent RPMI-8226 cells and RPMI-8226/TP-110 cells were incubated in fresh medium for 24 h, and total RNA was then extracted from the control (parent) and the experimental (resistant) cells. The changes in mRNA expression in the RPMI-8226/TP-110 cells are shown in Table 3. *ABCB1*, *FLJ10178*, *HSPB8*, *CCL2*, *AUTS2*, *RPIB9*, *ZNF521*, *CYP24A1*, *CFC1*, and *BTBD3* showed increased expression in the resistant cells, while *FN1*, *SLC27A2*, *TOM1L1*, *EPDR1*, *CADPS2*, *KIAA0802*, *STARD3NL*, *HMGA2*, *FLJ14564*, and *DMRT2* showed decreased expression. Among those genes showing altered expression, *ABCB1* is known to be involved in MDR. The expression levels of 44 ABC transporter genes are shown in Table 4. Among the ABC transporters examined, only *ABCB1* showed higher expression. This suggests that the ABCB1 transporter is profoundly involved in the mechanism of drug resistance in RPMI-8226/TP-110 cells.

Expression of ABCB1 in RPMI-8226/TP-110 cells

Expression of ABCB1 in the RPMI-8226/TP-110 cells was confirmed by RT-PCR and Western blotting. ABCB1 expression was markedly elevated in these cells, but the expression of ABCC1 (MRP1) was not elevated as to mRNA and protein levels (Fig. 4A and B).

Effects of ABC transporter inhibitors on RPMI-8226/TP-110 cells

In order to determine whether the ABCB1 transporter is involved in the resistance mechanism in the RPMI-8226/TP-110 cells, we examined the effects of an ABC transporter inhibitor. The addition of verapamil, well-known to be an ABC transporter antagonist, reversed not only TP-110 resistance, but also the MG-132, bortezomib, and doxorubicin resistance in the RPMI-8226/TP-110 cells (Table 5). Additionally, we examined the effects of other MDR1 inhibitors and other a Ca^{2+} antagonists, because verapamil has the effect of a Ca^{2+} antagonist. In results, MDR1 inhibitors (cyclosporin A and qunidine) reversed TP-110 resistance, but Ca^{2+}

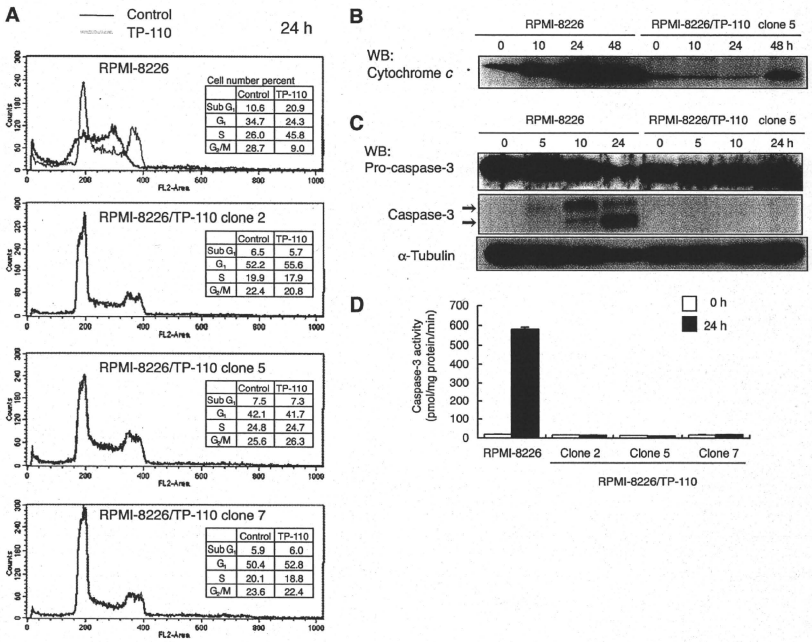

Fig. 3. Characteristics of the RPMI-8226/TP-110 Cells.

Cells were incubated with 0.1 μg/ml TP-110. A, After 24 h, the cells were examined by flow cytometry. B, Cells were incubated with 0.1 μg/ml TP-110. After 10, 24, and 48 h, the cytosol fraction of the cells was extracted using digitonin lysis buffer. C, After 24 h, Western blot analysis was performed using whole cell lysates, as described in "Materials and Methods." D, After 24 h, the caspase-3 activity of whole-cell lysates was assessed as described in "Materials and Methods."

antagonists (diltiazem and nifedipine) did not (Supplemental Table 1; see *Biosci. Biotechnol. Biochem.* Web site). This suggests that resistance in RPMI-8226/TP-110 cells depends on the expression of ABCB1.

Effects of TP-110 on the K-562/DOX cells

Resistance to TP-110 in another cell line that expresses ABCB1 was then investigated. K-562/DOX cells showed high expression of ABCB1, but K-562 (parent) cells did not (Supplemental Fig. 1; see *Biosci. Biotechnol. Biochem.* Web site). Predictably, the K-562/DOX cells showed strong resistance to TP-110. With regard to other proteasome inhibitors, K-562/DOX cells showed resistance to MG-132 and bortezomib, similarly to the RPMI-8226/TP-110 cells, while they were not resistant to lactacystin (Tables 2 and 6).

Discussion

In cancer drug discovery, the proteasome is a promising molecular target.[5] In addition to the treatment of relapsed or refractory multiple myeloma, bortezomib is also undergoing clinical trials for the treatment of several cancers (*e.g.*, prostate).[20] TP-110 (Fig. 1) strongly inhibits the growth of various human cell lines and induces apoptosis in their cells.[12] In order to strengthen its therapeutic effects, we established RPMI-8226/TP-110 cells and elucidated their resistance mechanisms.

Our results suggest that the factor involved in resistance of the RPMI-8226/TP-110 cells is *ABCB1*. DNA microarray is a useful tool to estimate changes in gene expression in cells. Our analytical results indicate that *ABCB1* is overexpressed in RPMI-8226/TP-110 cells (Table 3). The results of Western blotting and RT-PCR support the results of DNA microarray analysis. The addition of verapamil (10 μg/ml) reversed resistance in RPMI-8226/TP-110 cells (Table 5). Furthermore, K-562/DOX cells expressing ABCB1 also showed strong resistance to TP-110 as compared to MG-132 and bortezomib (Table 6). This suggests that RPMI-8226/TP-110 cells expressing ABCB1 (MDR1) are incidentally isolated in the exposure of TP-110 to RPMI-8226 cells, and acquire cross-resistance to antitumor drugs. K-562/DOX show similar cross-resistance to TP-110 and doxorubicin, suggesting that TP-110 is effluxed by the same mechanism as doxorubicin. Neither the RPMI-8226/TP-110 cells nor the K-562/DOX cells

Table 3. Gene Expression Changes in RPMI-8226/TP-110 Cells

Increased expression of mRNA in RPMI-8226/TP-110

Gene name	Gene symbol	$\log_2$ of expression ratio
ATP-binding cassette, sub-family B (MDR/TAP), member 1	*ABCB1*	5.89
Hypothetical protein FLJ10178	*FLJ10178*	5.82
Heat shock 22 kDa protein 8	*HSPB8*	5.34
Chemokine (C-C motif) ligand 2	*CCL2*	5.28
Autism susceptibility candidate 2	*AUTS2*	4.97
Rap2 binding protein 9	*RPIB9*	4.87
Zinc finger protein 521	*ZNF521*	4.82
Cytochrome P450, family 24, subfamily A, polypeptide 1	*CYP24A1*	4.72
Crypto	*CFC1*	4.41
BTB (POZ) domain containing 3	*BTBD3*	4.37

Decreased expression of mRNA in RPMI-8226/TP-110

Gene name	Gene symbol	$\log_2$ of expression ratio
Fibronectin 1, transcript variant 1	*FN1*	−6.17
Soluble carrier family 27 (fatty acid transporter), member 2	*SLC27A2*	−5.79
Target of myb1-like 1 (chicken)	*TOM1L1*	−5.66
Ependymin related protein 1 (zebrafish)	*EPDR1*	−5.47
Ca^{2+}-dependent activator protein for secretion 2	*CADPS2*	−5.37
KIAA0802	*KIAA0802*	−5.09
STARD3 N-terminal like	*STARD3NL*	−5.04
High mobility group AT-hook2	*HMGA2*	−4.92
Hypotherical protein FLJ14564	*FLJ14564*	−4.91
Doublesex and meb-3 related transcription factor 2	*DMRT2*	−4.85

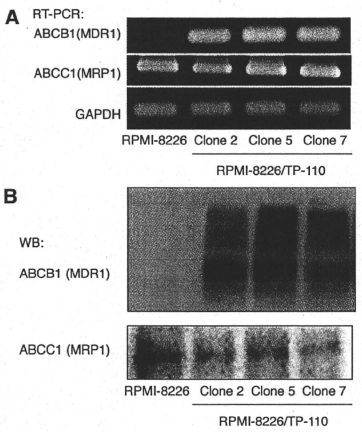

Fig. 4. Expression of ABCB1 and ABCC1 in RPMI-8226/TP-110 Cells.

RPMI-8226 and RPMI-8226/TP-110 cells were incubated for 24 h. A, *ABCB1* and *ABCC1* mRNA expression was assessed by RT-PCR. B, ABCB1 and ABCC1 protein expression was assessed by Western blot analysis.

were resistant to lactacystin. This susceptibility depends on the physico-chemical properties of the compound, including its hydrophobicity and molecular weight.[21,22]

Resistance to chemotherapeutic agents is a significant problem in the treatment of cancer.[14] Colchicine, doxorubicin, etoposide, vinblastin, and paclitaxel are frequently effluxed by P-gp in resistant tumor cells. RPMI-8226/TP-110 cells expressing ABCB1 (MDR1) are incidentally isolated by the exposure of RPMI-8226 cells to TP-110, though their cells do not express ABCC1 (MRP1) (Table 4), and thus RPMI-8226/TP-110 cells show cross-resistance to various anti-tumor drugs. Accordingly, TP-110 exhibits potent anti-tumor activity *in vitro* but continuous administration of TP-110 to mice is assumed to induce expression of P-gp.

On DNA microarray analysis, 44 ABC transporters were investigated. As shown in Table 4, *ABCB1* was strongly overexpressed and *ABCG1* was slightly over-expressed in RPMI-8226/TP-110 cells. Conversely, *ABCG8* was repressed in the RPMI-8226/TP-110 cells. *ABCG1* is reported to regulate the functions of macrophage cholesterol and phospholipid transport in Drosophila,[18] but the functions of these genes in humans are not known.

Drug resistance can be avoided by inhibiting the function of transporters induced by chemotherapy. Verapamil in breast cancer and non-small cell lung carcinoma and cyclosporin A in acute myeloid leukemia have shown benefits in clinical trials.[23] A third generation of inhibitors, including PSC833 and MS-209, are now being developed.[19] Therefore, combination therapy with TP-110 and an ABCB1 inhibitor might produce beneficial effects *in vivo*.

Inconsistent findings involving proteasome inhibitors and P-gp have been reported. Bortezomib and MG-132, proteasome inhibitors, reportedly reduced the degree of the MDR in MCF-7/DOX cells,[24] and MG-132 apparently reversed the MDR of gastric cancer by inhibiting P-gp.[25] These findings suggest that proteasome inhibitors attenuate the expression of P-gp and induce

Table 4. Expression of ABC Transporter Genes in RPMI-8226/TP-110 Cells

Gene symbol	Sub-family	$\log_2$ of expression ratio
ABCA1	ABC1	−0.19
ABCA2	ABC1	0.52
ABCA4	ABC1	0.00
ABCA5	ABC1	0.06
ABCA6	ABC1	−0.24
ABCA7	ABC1	−0.28
ABCA8	ABC1	0.00
ABCA9	ABC1	0.53
ABCA10	ABC1	−0.18
ABCA12	ABC1	0.39
ABCB1	MDR/TAP	5.89
TAP1	MDR/TAP	0.50
TAP2	MDR/TAP	0.45
ABCB4	MDR/TAP	0.59
ABCB5	MDR/TAP	0.00
ABCB6	MDR/TAP	−0.04
ABCB7	MDR/TAP	0.13
ABCB8	MDR/TAP	0.39
ABCB9	MDR/TAP	−0.05
ABCB10	MDR/TAP	0.06
ABCB11	MDR/TAP	0.19
ABCC1	CFTR/MRP	−0.31
ABCC2	CFTR/MRP	1.09
ABCC3	CFTR/MRP	0.11
ABCC4	CFTR/MRP	−0.44
ABCC5	CFTR/MRP	0.71
ABCC6	CFTR/MRP	−0.26
CFTR	CFTR/MRP	−0.22
ABCC8	CFTR/MRP	0.47
ABCC9	CFTR/MRP	0.80
ABCC10	CFTR/MRP	0.73
ABCC11	CFTR/MRP	−0.36
ABCC12	CFTR/MRP	0.00
ABCC13	CFTR/MRP	0.00
ABCD2	ALD	0.36
ABCD3	ALD	−0.01
ABCE1	OABP	−0.34
ABCF1	GCN20	0.57
ABCF2	GCN20	0.14
ABCG1	WHITE	1.92
ABCG2	WHITE	−0.55
ABCG4	WHITE	0.59
ABCG5	WHITE	0.00
ABCG8	WHITE	−3.02

Table 5. Effects of Verapamil on RPMI-8226/TP-110 Cells

Verapamil (10 μg/ml)	IC_{50} (μg/ml)			
	RPMI-8226		RPMI-8226/TP-110 clone 5	
	−	+	−	+
TP-110	0.030	0.028	0.37 (12.3*)	0.053 (1.8)
MG-132	0.50	0.28	1.9 (3.8)	0.48 (0.96)
Bortezomib	0.0019	0.0019	0.0030 (1.6)	0.0019 (1.0)
Doxorubicin	0.0037	0.014	1.1 (297)	0.11 (30)

*Values in parentheses indicate index of resistance (fold).

apoptosis in resistant tumor cells. On the other hand, the proteasome inhibitors bortezomib and MLN273 are substrates of P-gp in leukemic cells, and knockdown of P-gp resensitizes cells against these inhibitors.[26] Ohkawa *et al.* reported a possible role of calpain in P-gp turnover.[27] In the RPMI-8226/TP-110 cells, our results clearly indicate that a proteasome inhibitor, TP-110, is the substrate of ABCB1 (P-gp).

Table 6. Effects of TP-110 on Doxorubicin-Resistant K-562/DOX Cells

	IC_{50} (μg/ml)	
	K-562	K-562/DOX
TP-110	0.053	4.8 (91*)
MG-132	1.6	5.1 (3.0)
Bortezomib	0.0093	0.037 (4.0)
Lactacystin	0.44	0.40 (0.90)
Doxorubicin	0.046	2.8 (60)

*Values in parentheses indicate index of resistance (fold).

In conclusion, results of the present study indicate that the resistance factor in established RPMI-8226/TP-110 cells is *ABCB1*. Overexpression of ABCB1 in the RPMI-8226/TP-110 cells was indicated by the results of DNA microarray analysis, and was supported by the results of RT-PCR and Western blotting. Moreover, the addition of an ABCB1 inhibitor, verapamil, reversed resistance in the RPMI-8226/TP-110 cells. These results suggest that TP-110 therapy requires such inhibitors to overcome resistance *via* P-gp. Chemical modification of TP-110 and/or combination therapy with an ABCB1 inhibitor is a promising approach in cancer chemotherapy.

Acknowledgment

This work was supported by the Ministry of Health, Labor, and Welfare of Japan as part of the Third-Term Comprehensive Ten Year Strategy for Cancer Control.

References

1) Adams J, *Nat. Rev. Cancer*, **4**, 349–360 (2004).
2) Chauhan D, Hideshima T, and Anderson KC, *Annu. Rev. Pharmacol. Toxicol.*, **45**, 465–476 (2005).
3) Almond JB and Cohen GM, *Leukemia*, **16**, 433–443 (2002).
4) Adams J, Behnke M, Chen S, Cruickshank AA, Dick LR, Grenier L, Klunder JM, Ma YT, Plamondon L, and Stein RL, *Bioorg. Med. Chem. Lett.*, **8**, 333–338 (1998).
5) Orlowski RZ and Kuhn DJ, *Clin. Cancer Res.*, **14**, 1649–1657 (2008).
6) Kane RC, Bross PF, Farrell AT, and Pazdur R, *Oncologist*, **8**, 508–513 (2003).
7) Momose I, Sekizawa R, Hashizume H, Kinoshita N, Homma Y, Hamada M, Iinuma H, and Takeuchi T, *J. Antibiot.*, **54**, 997–1003 (2001).
8) Momose I, Sekizawa R, Hirosawa S, Ikeda D, Naganawa H, Iinuma H, and Takeuchi T, *J. Antibiot.*, **54**, 1004–1012 (2001).
9) Momose I, Sekizawa R, Iinuma H, and Takeuchi T, *Biosci. Biotecnol. Biochem.*, **66**, 2256–2258 (2002).
10) Momose I, Umezawa Y, Hirosawa S, Iinuma H, and Ikeda D, *Bioorg. Med. Chem. Lett.*, **15**, 1867–1871 (2005).
11) Momose I, Umezawa Y, Hirosawa S, Iijima M, Iinuma H, and Ikeda D, *Biosci. Biotechnol. Biochem.*, **69**, 1733–1742 (2005).
12) Momose I, Iijima M, Kawada M, and Ikeda D, *Biosci. Biotechnol. Biochem.*, **71**, 1036–1043 (2007).
13) Iijima M, Momose I, and Ikeda D, *Anticancer Res.*, **29**, 977–985 (2009).
14) Tsuruo T, Naito M, Tomida A, Fujita N, Mashima T, Sakamoto H, and Haga N, *Cancer Sci.*, **94**, 15–21 (2003).
15) Dean M, Fojo T, and Bates S, *Nat. Rev. Cancer*, **5**, 275–284 (2005).
16) Cole SP, Bhardwaj G, Gerlach JH, Mackie JE, Grant CE, Almquist KC, Stewart AJ, Kurz EU, Duncan AM, and Deeley RG, *Science*, **258**, 1650–1654 (1992).
17) Doyle LA, Yang W, Abruzzo LV, Krogmann T, Gao Y, Rishi AK, and Ross DD, *Proc. Natl. Acad. Sci.*, **95**, 15665–15670 (1998).